JUN 18 1971

AEDC-TR-71-99

NOV 19 1971
JUN 18 1985
SEP 26 1989

copy 2

ENVIRONMENTAL TESTS OF
METEOROLOGICAL RADIOSONDES INCLUDING
DYNAMIC TEMPERATURE AND HUMIDITY SIMULATION
IN A WIND TUNNEL

R. S. Hiers

ARO, Inc.

June 1971

TECHNICAL REPORTS
FILE COPY

VON KÁRMÁN GAS DYNAMICS FACILITY
ARNOLD ENGINEERING DEVELOPMENT CENTER
AIR FORCE SYSTEMS COMMAND
ARNOLD AIR FORCE STATION, TENNESSEE

NOTICES

ENVIRONMENTAL TESTS OF
METEOROLOGICAL RADIOSONDES INCLUDING
DYNAMIC TEMPERATURE AND HUMIDITY SIMULATION
IN A WIND TUNNEL

R. S. Hiers

ARO, Inc.

FOREWORD

The work reported herein was done at the request of the Air Weather Service (AWS) under Program Element 35111F.

The results of tests presented herein were obtained by ARO, Inc. (a subsidiary of Sverdrup & Parcel and Associates, Inc.), contract operator of the Arnold Engineering Development Center (AEDC), Air Force Systems Command (AFSC), Arnold Air Force Station, Tennessee, under Contract F40600-71-C-0002. The tests were conducted during the period from September 23 to November 20, 1970, in Tunnel D, von Kármán Gas Dynamics Facility (VKF), under ARO Project No. VT0131. The manuscript was submitted for publication on March 5, 1971.

The author wishes to acknowledge the assistance of Richard W. Rhudy, ARO, Inc., and Lt. Brian P. Severin, AWS, during these tests.

This technical report has been reviewed and is approved.

Emmett A. Niblack, Jr.
Lt Colonel, USAF
AF Representative, VKF
Directorate of Test

Joseph R. Henry
Colonel, USAF
Director of Test

ABSTRACT

An experimental investigation of the performance of meteorological radiosondes subjected to controlled variations of humidity and temperature in an environmental wind tunnel is described. Dynamic variations in temperature between -60 and 40°C and in relative humidity between 0 and 100 percent, representative of those encountered in atmospheric flight, were simulated by injecting liquid nitrogen or steam, respectively, into the wind-tunnel air supply. Tests were conducted at free-stream velocities of 15 and 75 ft/sec duplicating the average ascent and descent rates, respectively, of balloon-borne rawinsondes and dropsondes. Free-stream static pressures appropriate to the 300- and 700-mb levels were employed. Results showed that radiosonde temperature instrumentation was generally quite accurate. Corresponding humidity instrumentation also yielded satisfactory results except in the presence of direct water droplet impingement or operational equipment malfunction.

CONTENTS

APPENDIXES

I. ILLUSTRATIONS

Figure

NOMENCLATURE

e	Base of the natural logarithm system, $e = 2.718$
f	Temperature-pressure saturation relation for water (See Section 2.3.4)
p	Pressure, psia
RH	Relative humidity, percent RH (See Section 2.3.4)
T	Temperature, °C
u	Velocity, ft/sec
Δp	Pitot-static pressure difference, psi
τ	Response time, sec, (See Fig. 6)

SUBSCRIPTS

∞	Test section free-stream conditions
DP	CRL hygrometer mirror conditions

SUPERSCRIPT

'   ·   Water vapor partial pressure

Metric and English systems were utilized so that parameters of direct meteorological and test facility operational interest would be cast in appropriate units.

SECTION I
INTRODUCTION

A series of unique environmental tests designed to provide information for evaluating statistical accuracy and time-response characteristics of the temperature, humidity, and pressure instrumentation of selected sets of operational meteorological radiosondes is described.

The performance of balloon-borne J00X-series rawinsondes and AMT-13 dropsondes was investigated in a supersonic wind tunnel specially modified for subsonic operation at nominal free-stream velocities of 15 and 75 ft/sec, which duplicated the average ascent and descent rates, respectively, of the rawinsondes and dropsondes. Ambient free-stream temperature, humidity, and pressure variations representative of typical atmospheric conditions encountered at the 300- and 700-millibar (mb) levels (nominally 30,000 ft and 10,000 ft, respectively) were simulated in the test section by mixing liquid nitrogen and steam with the wind-tunnel air supply.

Water droplets generated in the flow provided a means for evaluating the effects of rain or cloud encounters on sonde performance. Additional test requirements for prescribed "step changes" in test section temperature and relative humidity were not necessary for evaluating radiosonde performance and were relaxed somewhat.

A high degree of free-stream temperature and relative humidity uniformity was essential for the conduct of the test since radiosonde performance was evaluated by comparison with simultaneous wind-tunnel measurements. Likewise, wind-tunnel instrument accuracy and precision, substantially better than the corresponding radiosonde instrumentation, were also required. These features of the test section performance were demonstrated during an extensive facility calibration.

Radiosonde testing was concentrated on humidity and temperature measurements to realize full advantage of the novel capability of the facility to convect time-dependent simulated atmospheric samples through the test section. Characteristics of the radiosonde pressure transducers which can be readily determined in a static pressure chamber were not fully explored.

The scope of this document is limited to describing the modifications, operation, and performance of the test facility, summarizing the radiosonde experiments, and presenting typical radiosonde results. Statistical evaluation of radiosonde performance is beyond the scope of this test

report, although certain qualitative aspects of radiosonde characteristics are discussed.

SECTION II
APPARATUS

2.1 RADIOSONDES

Photographs of representative samples from the sets of AMT-13 dropsondes and J00X-series rawinsondes provided by AWS for these tests are presented in Figs. 1 and 2, Appendix I, respectively. The thermistor and hygristor elements of each-type radiosonde, as well as the corresponding ventilation paths, are shown in these photographs. The dropsondes and rawinsondes normally employ the externally similar "ML-476"- and "CM"-type humidity elements, respectively, illustrated in Figs. 1 and 2. The extraneous wires attached to the dropsonde sensor board were used for selective commutation during the tests. The thermistor and hygristor element resistances were functions of temperature, and of temperature and humidity, respectively, and were commutated in a common circuit that converted resistance to frequency in the audio spectrum for pulse-modulating a radio frequency transmitter.

Transfer equations relating nominal element design resistance to radiosonde "audio" frequency and thence to temperature and relative humidity were provided by AWS for data reduction purposes. In addition, an environmental calibration chamber was also supplied for "baselining" these resistive elements prior to testing. The baseline equipment was used to measure the actual resistance of each element at a certain environmental condition and subsequently to determine a "correction factor" for use with the transfer equations.

For these tests, regulated power supplies were substituted for normal radiosonde battery power and additional modifications included provision for bypassing the transmitter and detecting audio frequency signals at the transmitter input. Several dropsondes were modified by the addition of an improvised precipitation shield described later.

2.2 TEST FACILITY

Tunnel D is an intermittent, variable density wind tunnel with a manually adjusted, flexible-plate-type nozzle and a 12- x 12-in. test

section. The wind tunnel normally is operated at supersonic speeds with an air working medium supplied through automatic throttling valves from a high-pressure storage system and discharged into a large vacuum sphere. A description of the wind tunnel and its conventional operating characteristics may be found in the Test Facilities Handbook[1].

For the present environmental tests, the wind tunnel was operated at free-stream velocities of 15 and 75 ft/sec by establishing sonic flow through a partially opened control valve downstream of the test section and by setting the flexible nozzle plates at the maximum available throat area, thereby eliminating the conventional sonic throat section. Ambient pressure in the test section was regulated at 4.35 and 10.0 psia (300 and 700 mb, respectively) by appropriately throttling the air from the high-pressure supply. Test velocity was nominally independent of ambient pressure and was a function primarily of the ratio of test section to downstream sonic cross-sectional area and was established by merely opening the downstream control valve to a predetermined setting. A schematic diagram, illustrating various features of the test facility, is shown in Fig. 3.

Additional modifications to the conventional wind-tunnel circuit included the installation of mixing chambers upstream of the stilling chamber. Both mixing chambers were internally baffled to enhance homogeneous mixing of the steam and/or nitrogen with the air supply. Superheated steam (200°C and 50 psia) was throttled into the mixing chamber as illustrated in Fig. 3 to provide controlled variations in test section relative humidity. Similarly, liquid nitrogen from a 35-psia regulated supply was flashed just downstream of the control valve prior to entering the mixing chamber to provide a means of controlling the test section ambient temperature.

The normal screen section in the stilling chamber was removed to prevent damage in the event of icing and was replaced with a baffle system and liner to promote uniformity in the test section properties.

The relatively low mass flow rates required in conjunction with the continuous pumping capacity provided by the VKF compressor plant resulted in essentially continuous flow operation during these tests.

---

[1]Test Facilities Handbook (Eighth Edition). "Von Karman Gas Dynamics Facility, Vol. 4." Arnold Engineering Development Center, December 1969 (AD863646).

Typical operational procedures consisted of initially adjusting the downstream control valve to the setting appropriate to the selected velocity and then adjusting the upstream throttling valve to establish flow at the desired ambient pressure. Steam or liquid nitrogen was subsequently introduced to generate the desired conditions of ambient temperature and relative humidity. During the addition of steam or liquid nitrogen, ambient pressure was maintained constant by simultaneously adjusting throttling valves from the high-pressure air supply. Since free-stream velocity was relatively insensitive to free-stream temperature and humidity, the downstream control valve was not adjusted during nitrogen or steam injection.

A photograph of a typical dropsonde installation, taken from the vicinity of the stilling chamber illustrating the relatively constant nozzle cross-sectional area, is presented in Fig. 4. Note that the port sidewall has been retracted from the nozzle for this photograph. Unless otherwise indicated, radiosonde and wind-tunnel instrument sensors were normally installed at the upstream limit of the conventional test section region.

2.3 INSTRUMENTATION

Voltage signals from the wind-tunnel and radiosonde instrumentation systems described in this section were amplified, digitized, and recorded on magnetic tape at the rate of four times per second with a low noise data acquisition system assembled for these tests. Repeatability and long term stability of this system were equivalent to $\pm 3\,\mu v$ referenced to the input. A separate data acquisition system employing an analog magnetic tape recorder was utilized during initial testing but was discarded because of unacceptable precision limitations associated with system noise.

Calibration of the digital data system was periodically verified using a standard voltage cell in conjunction with a Leeds and Northrop model K-3 precision potentiometer and typically was found accurate to within $\pm 3\,\mu v$ referenced to the input. With the exception of free-stream temperature uncertainty, which is evaluated in a succeeding section, the accuracy and precision limitation of the data acquisition system had negligible effect on the uncertainties associated with instrumentally derived parameters.

Estimates of the random uncertainty of instrumentation in this section generally represent bands containing the residuals of 99 percent of the corresponding observations, except that the residuals of all observations were included where limited calibration data were available.

2.3.1 Pressure

The inferred test section ambient pressure was measured in the stilling chamber with standard Tunnel D stagnation pressure instrumentation which consisted of a 60-psia transducer operated on a full-scale calibrated range of 20 psia. Random uncertainties associated with the pressure instrumentation for the present test conditions (±0.5 percent) have been established from previous calibrations including periodic comparisons with secondary standards. It is noted that the pressure differences between the test section and the stilling chamber were usually less than instrument derived pressure uncertainty, thus justifying the approximation that these pressures were equivalent for the purposes of this test. Since test section ambient pressure was maintained nominally constant, pressure instrumentation time response was not evaluated.

2.3.2 Temperature

Free-stream temperature was measured in the test section with either relatively "slow" or "fast" time-response thermocouple probes (referenced to a distilled water ice bath) which were designed and calibrated for these tests. Six "fast" time-response thermocouples were constructed by joining 0.005-in.-diam Chromel®[2]-Alumel®[2] wires essentially end-to-end with the minimum required silver solder. The resulting junctions were stretched between two supports (1/4 in. apart) and mounted in the test section with the wire axis perpendicular to the free-stream flow. Four of these "fast" time response thermocouple probes, referred to as cylindrical thermocouple probes, were calibrated with platinum resistance thermometer equipment traceable to the Bureau of Standards to an estimated accuracy of ±0.05°C. Random uncertainties of ±0.05°C were attributed to both the repeatability and the calibration of the data recording system. Typical operational errors related to wire support conduction and tunnel wall radiation of ±0.05°C have also been estimated. The total uncertainty characterizing temperature measurements obtained with these probes was conservatively estimated to have been ±0.25°C by directly summing these various contributions.

Two relatively slow time-response thermocouples, designated as spherical thermocouple probes, were constructed by forming a bead of silver solder approximately 0.03 in. in diameter around the ends of 0.012-in.-diam copper-constantan wires which had been twisted together. The individual contributions to the instrument uncertainty of

---

[2]Registered tradenames of Hoskins Mfg. Co., Detroit, Michigan.

these probes were not separately evaluated, although the total uncertainty was estimated by comparing the results obtained from the cylindrical and spherical probes in a common environment. Representative results obtained with each thermocouple mounted in the test section under evacuated, no-flow conditions illustrate (Fig. 5) that the uncertainties of each thermocouple probe are essentially equivalent. In summary, the total uncertainty associated with all steady-state temperature measurements is estimated to have been ±0.25°C.

Time-response characteristics of each type of thermocouple probe and a dropsonde thermister were evaluated by resistively heating each sensor element to approximately 5 to 10°C above the local ambient temperature at each test velocity and pressure, and then observing the temperature-time decay of the sensors when the heating current was suddenly removed. Time response of each sensor could be formulated in terms of a simple "time constant" since the local film coefficient was essentially constant and because the internal thermal resistance of each sensor was small compared to the corresponding surface resistance. A typical time-response measurement and a summary of time constant values, defined conventionally as the time required for the fraction $1/e$ of the temperature change to occur, are illustrated in Fig. 6. The relative insensitivity of thermister time response to velocity and pressure is a characteristic typical of the radiosonde temperature and relative humidity instrumentation.

2.3.3 Velocity

Test section free-stream velocity was derived from the steady-state Bernoulli equation for air

$$u_\infty = \left\{ 6190 \, (\Delta p/p_\infty) \, (T_\infty + 273) \right\}^{1/2}, \text{ ft/sec}$$

where Δp is the difference between local stagnation and static pressures, and was measured with a 1-psid MKS Baratron®[3] pressure transducer system. The pressure difference was determined by detecting the pressure differential between either the tunnel stilling chamber and test section wall or a test section pitot probe and test section wall. Wall static pressure was sensed approximately 4 in. upstream of the axial station where radiosonde sensor elements were located. Nominal pressure differences associated with each velocity are listed below with the corresponding random uncertainty of the MKS Baratron instrumentation.

---

[3]Registered tradename of MKS Instruments, Inc., Burlington, Massachusetts.

u_∞, ft/sec	p_∞, psia	Δp, psi	Δp Uncertainty, psi
15	4.35	0.00054	0.00001
	10.0	0.00124	0.00003 ·
75	4.35	0.0135	0.0003
	10.0	0.031	0.001

The random uncertainty in velocity calculated by propagating individual contributions in Δp, T_∞, and p_∞ through the Bernoulli relationship is dominated by the stagnation-static pressure difference term. Therefore, the velocity itself was considered as an independent, instrumentally derived parameter in evaluating test section characteristics. The corresponding effective random uncertainty of the "velocity measurement" was estimated to have been less than ±1.5 percent. Other dominating uncertainties in free-stream velocity, including the consequence of formulating velocity in terms of the steady-state Bernoulli equation, are discussed in a later section.

2.3.4 Relative Humidity

Test section relative humidity was calculated from the corresponding dewpoint temperature measured with a Cambridge Research Laboratory (CRL) model 992 dewpoint hygrometer supplied continuously with a sample of test section flow through 1/4-in. stainless steel tubing. A portion of the test section sample was exhausted through an auxiliary vacuum pump which served as a water droplet trap and aided in establishing maximum pumping speed (and hence time response) consistent with a minimum pressure drop in the supply tube. Essentially, the entire length of the supply tube was heated to approximately 50°C to minimize sample condensation.

The CRL dewpoint hygrometer is a primary standard instrument, requiring no additional laboratory calibration, which cools a sample of moist air at constant pressure until condensation is observed on a mirror in thermal equilibrium with the sample. The dewpoint temperature, so established, was detected by a calibrated copper-constantan thermocouple implanted in the mirror and referenced to a distilled water ice bath.

Test section relative humidity was calculated from the relationship

$$RH = 100 \, \frac{p'(T_{DP})}{p'(T_\infty)} \, \frac{p_\infty}{p_{DP}} \, , \text{ percent RH}$$

which can be expressed functionally as

$$RH = \frac{f(T_{DP})}{f(T_\infty)} \frac{p_\infty}{p_{DP}}$$

where f represents the temperature-pressure relationship for equilibrium saturation between water vapor and liquid. T_∞ and p_∞ were obtained from the previously described instrumentation and were characterized by representative random uncertainty contributions of ±0.1°C and ±0.5 percent, respectively. Random instrument uncertainties of ±0.15°C (including manufacturer's specifications for mirror temperature gradients) and ±1 percent have been estimated for the dewpoint temperature (T_{DP}) and the dewpoint total pressure (p_{DP}) measurements. Representative random uncertainties of ±1.5 percent in the effective relative humidity measurement, which is considered to have been an independent instrumentally derived parameter, were estimated by propagating the individual uncertainty contributions through the above data reduction equation under the assumption that individual errors combined randomly.

A fixed bias error as high as ±3.5 percent in relative humidity has been estimated from the manufacturer's tolerance of ±0.6°C on thermocouple accuracy. The total pressure ratio term in the above equation contributed negligible fixed bias error to the relative humidity calculation since the pressure transducers were simultaneously calibrated near the appropriate operating pressures. Similarly, free-stream temperature measurements obtained with the calibrated thermocouple probes contributed negligible fixed error.

The total uncertainty in steady-state relative humidity measurements obtained with the CRL instrumentation was estimated, by summing the random and fixed error contributions, to have been ±5 percent. Initial calibration of the CRL instrumentation with samples of known relative humidity and comparisons with other humidity instrumentation indicated that the estimated fixed error in relative humidity may be unrealistically severe, although more representative values have not been fully documented.

Manufacturer's specifications indicate the CRL dewpoint hygrometer instrumentation should respond accurately to linear time rates of change in dewpoint temperature of 3°C/sec and that response to within 63 percent of a 10°C step change should occur within three seconds. Operational experience has shown, however, that overall system time response was considerably slower, partly because of the associated supply tubing, and hence the dewpoint hygrometer was used chiefly for determining quasi-steady-state relative humidity levels.

A Panametrics, Inc. (PI) model 1000 hygrometer, operated in an uncalibrated mode, was used for evaluating the effects of liquid water drops on radiosonde performance. The PI sensor, which consisted of a durable, gold-plated aluminum oxide matrix that absorbed moisture in proportion to the ambient water vapor partial pressure, was mounted directly in the flow near the downstream limit of the conventional test section and was exposed to the same flow environment as the radiosondes. The radiosonde and the PI sensors operated on similar physical principles, although the PI sensor provided a variable capacitance element in the detecting circuit and the radiosonde hygrister provided a resistive element. The PI instrument signal was functionally related to dewpoint temperature within an estimated random uncertainty equivalent to ±0.5°C based on manufacturer's specifications.

2.3.5 Radiosonde

The audio frequencies generated by the radiosondes which normally pulse modulate a radio frequency transmitter were detected at the input to the transmitter during these tests. The audio frequency signals were converted to analog voltages for data processing and recording. A calibrated frequency counter provided a standard for the frequency to voltage converters. The effective total uncertainty introduced into the audio frequency by the signal conditioning equipment peculiar to these tests is estimated to have been ±2 and ±0.2 Hz, respectively, for the dropsonde and rawinsonde tests. The corresponding uncertainties in temperature and relative humidity derived from radiosonde transfer equations are estimated to have been ±0.10°C and ±0.4 percent RH, respectively, for representative conditions.

The effects of a separate source of error in calculated radiosonde relative humidity values, peculiar to the wind-tunnel tests, arose from the substitution of tunnel free-stream temperature for radiosonde temperature measurements in the transfer equations. The uncertainty in radiosonde relative humidity traceable directly to the total uncertainty of ±0.25°C in the wind-tunnel static temperature measurement is estimated to have been ±0.1 percent RH.

SECTION III
TEST SECTION CALIBRATION

3.1 VELOCITY AND PRESSURE

Free-stream velocity characteristics were evaluated with pitot probe measurements made at two separate lateral locations in the plane

of the axial test station. Additionally, an effective average test section velocity was also derived from stilling chamber total-pressure measurements during some runs to aid in assessing velocity uniformity. Velocity-time histories obtained during typical dropsonde and rawinsonde experiments, for test conditions incorporating liquid-nitrogen and steam injection, are shown in Fig. 7. Digitized time histories were originally machine plotted by connecting data at each 0.25-sec time interval. The resulting pseudo-analog displays were manually traced for presentation in this report.

The rapid decrease and subsequent gradual increase of mean velocity, illustrated in Fig. 7a for a representative nominal free-stream velocity of 75 ft/sec, resulted from controlled static temperature changes which were detected and accounted for in normal data reduction procedures at both free-stream velocities. Mean velocity variations of less than one percent associated with controlled relative humidity changes were considered insignificant and were not accounted for at either free-stream velocity.

Typical free-stream velocity characteristics obtained at a nominal 15-ft/sec velocity are illustrated in Fig. 7b. The large changes in velocity associated with changes in the rate of steam addition are attributed to the corresponding unsteady pressure wave system and are not representative of true velocity. Similar large velocity changes were also observed with liquid-nitrogen injection at 15 ft/sec.

The relatively high frequency velocity fluctuation observed at each free-stream velocity, and illustrated in Fig. 7, was attributed to air-flow turbulence and the resulting unsteady flow originating at the partially opened control valves. The bands in Fig. 7 show how the actual velocity unsteadiness could have been magnified merely by formulation of calculated velocity in terms of the steady-state Bernoulli equation. The band represents the maximum excursion about the mean velocity calculated according to one-dimensional theory[4] assuming an unsteady wave system located between the pitot and static pressure sources. Also, it should be pointed out that time-response limitations of the pressure difference instrumentation may also have invalidated velocity measurements associated with rapidly fluctuating pressures.

Based on the above considerations, it has been estimated that an uncertainty of approximately ±5 percent represents the velocity error

---

[4]Liepman, H. W. and Roshko, A. Elements of Gasdynamics. John Wiley and Sons, 1957, p. 79.

associated with flow unsteadiness for constant rates of liquid-nitrogen and steam injection. An examination of the limited lateral velocity profile information derived from individual time histories suggests that an uncertainty of ±5 percent represents the average test section velocity uniformity characteristics. The approximate uncertainty in typical velocity measurements for constant rates of liquid-nitrogen and steam injection was estimated to have been ±10 percent by summing the individual contributions attributed to flow unsteadiness and nonuniformity. Good agreement found between velocity measurements obtained with radiosondes, both installed and removed from the test section, indicated that distortion resulting from blockage was of little consequence and hence this aspect of the test section flow was not pursued further.

Although more exacting velocity uncertainty specifications could be documented for these tests, the preceding conservative estimates show that the data are not adversely affected since existing nonuniformity and unsteadiness were not detected as either significant errors in magnitude or phase in either free-stream or radiosonde temperature and humidity measurements.

Nominally constant ambient pressure histories in Fig. 8, corresponding to the preceding velocity measurements, illustrate the satisfactory pressure controllability achieved during steam and liquid-nitrogen injection. With the exception of large, operationally induced uncertainties, resulting from occasional grossly overcontrolled pressure fluctuations during liquid-nitrogen injection, ambient pressure uncertainties could typically be approximated by the associated instrument precision of ±0.5 percent.

3.2 TEMPERATURE

In addition to stringent accuracy and time-response requirements for free-stream temperature instrumentation, comparable lateral test section uniformity characteristics illustrated in this section were required by the simultaneous testing of as many as four radiosondes.

Representative time histories of free-stream temperature measured simultaneously at four test section locations with calibrated cylindrical thermocouple probes are shown in Fig. 9 for typical test conditions. The free-stream temperature variations are representative of conditions generated during the dropsonde and rawinsonde phase of testing. Figures 9a and b illustrate the inherent high degree of uniformity observed in the test section temperature at each nominal pressure level. Temperature measurements obtained with the four

cylindrical thermocouple probes, repositioned by rotation of the support-
ing strut (Fig. 9c), also display essentially indistinguishable time-
response and temperature correlation under steady-state and rapidly
varying conditions.

Test section temperature distribution measurements in Fig. 10
illustrate the effects of dropsonde flow fields on test section uniformity
characteristics and are equivalent to the results of Fig. 9. Test
section temperature distributions shown in Fig. 11, obtained with a
rawinsonde installed, also display no adverse effect of radiosonde flow
field on uniformity characteristics.

The total uncertainty in free-stream temperature measurements,
including instrumentation errors and nonuniformity and unsteadiness
of the test section flow, was estimated by comparing simultaneous
measurements (Figs. 9 through 11) to have been less than ±0.25°C. It
is noted that no operational limitations on the use of liquid-nitrogen
cooling were found and that the quoted free-stream temperature un-
certainty was applicable to essentially all time-dependent test condi-
tions generated during the tests.

3.3 RELATIVE HUMIDITY

The results of measurements documenting the performance and
uniformity characteristics of test section relative humidity distribu-
tions are described in this section. Results obtained by consecutively
sampling flow with the CRL dewpoint hygrometer, from several lateral
locations at the axial test station, are shown in Fig. 12 to illustrate
typical relative humidity uniformity characteristics under steady-state
conditions. Since simultaneous test section measurements were not
physically possible with the present wind-tunnel instrumentation, four
corresponding dropsonde time histories are presented in Fig. 13 to
illustrate relative humidity uniformity during rapid variations in the
rate of steam addition. From such results, test section relative
humidity was found to have been uniform to within approximately
±1.5 percent by comparing simultaneous measurements. Thus, the
total uncertainty in quasi-steady-state relative humidity measurements
with the CRL hygrometer was found to essentially equal the correspond-
ing instrumental uncertainties, which consisted of an estimated random
contribution of ±1.5 percent and a possible fixed bias of ±3.5 percent.

Although test section relative humidity remained uniform within
approximately ±1.5 percent during transients, the wind-tunnel mea-
surement itself was momentarily invalidated by time-response limita-
tion previously described in Section 2.3.4.

CRL and PI hygrometer data corresponding to the preceding drop-sonde measurements are compared in Fig. 14 to illustrate the quantitative response characteristics of each instrument. Time-response characteristics of the tunnel instrumentation precludes a determination of radiosonde time response from these experiments; however, a conservative limiting value can be obtained by assuming an instantaneous step change in test section relative humidity with steam control valve movement.

The preceding humidity characteristics are representative of tests where liquid water droplets were not present in the test section in substantial amounts. These conditions correspond to the majority of test results and include all data obtained at a velocity of 15 ft/sec. These conditions also correspond to data obtained at a velocity of 75 ft/sec where ambient temperature was maintained below 25°C, either naturally or artificially, with liquid-nitrogen injection.

The characteristically unique instrumentation response observed with relatively large quantities of water droplets in the test section is illustrated in Fig. 15. The presence of water droplets was most reliably detected by impingement on the thermocouple probes which was reflected through the data reduction equations as an apparent relative humidity fluctuation noted in Fig. 15. Condensation of steam in the relatively cool mixing chambers and subsequent transport of water droplets to the test section, suspended in partially saturated air, is attributed to large temperature differences between the mixing chambers and test section. This temperature difference, in conjunction with the higher flow velocity and corresponding short nozzle residence time, initially promoted condensation and then inhibited re-evaporation. The CRL hygrometer output was found to increase slowly with increasing steam injection in the presence of water droplets since it was responding essentially to the relative humidity of unsaturated air-water vapor mixture. Water contamination in the CRL hygrometer supply tube resulted in anomalous instrumental indication only during extended droplet impingement. The PI hygrometer, of course, responded primarily to the very high water vapor partial pressure resulting from direct droplet impingement.

Wind-tunnel operation with substantial quantities of water droplets in the test section was used primarily for qualitative indication of droplet impingement on radiosonde performance since droplet number density and size were not investigated.

SECTION IV
RADIOSONDE TESTS

4.1 TEST PROCEDURE

Dropsondes, rawinsondes, and corresponding sensor elements were selected or rejected utilizing operational AWS baseline tolerance criteria for radiosonde frequencies and sensor element resistances. Basic radiosonde and temperature elements were discarded when outside established baseline tolerances.

Dropsonde sensors were baselined in a standard environmentally controlled chamber using normal field operation techniques. The results of these procedures yielded nominal resistance of temperature or humidity sensors at a specific prescribed condition. "Correction factors" were formed for use in data reduction by ratioing the measured resistance values to the corresponding nominal design resistance values for these prescribed conditions. For simplicity, data reduction equations were formulated in terms of the nominal design resistance of the appropriate sensor element.

Equipment was provided only for manual rawinsonde data reduction with a "calculator wheel" appropriate to field baseline and data reduction techniques. Since this procedure was not suitable for wind tunnel use, an equivalent method was devised incorporating the standard environmental chamber for subjecting sensor elements to known conditions and an inverse procedure for inferring element "design" resistance from the normal rawinsonde transfer equations. Unfortunately, it was later determined that relative humidity conditions within the environmental chamber were erroneously detected by the baseline instrumentation. As a consequence, a similar baseline calibration procedure (substituting certain test section conditions measured with wind-tunnel instrumentation for the environmental chamber) was employed. Although the wind-tunnel and rawinsonde humidity data were therefore not independently derived, this alternative procedure was used to salvage otherwise questionable results.

Immediately prior to testing, radiosonde reference frequencies were recorded for data reduction purposes and the radiosondes were manually switched to provide a continuous signal from either the temperature or humidity element as desired. Following each run, reference frequencies were again recorded. Runs displaying significant reference frequency shifts were considered invalid. Normally, during flight, radiosondes are automatically commutated to provide reference

frequencies as well as temperature, humidity, and pressure signals at several discrete times per minute. Although greater potential accuracy is available by continuously updating reference frequencies in flight, the noncommutating mode employed during the wind-tunnel tests afforded considerable operational simplicity and permitted detailed resolution of sensor element time-response characteristics.

After velocity and pressure conditions had been established in the test section, the radiosondes were normally cycled through three temperature runs, each of approximately 10-min duration. Following these temperature tests, the radiosondes were commutated to provide a signal from the humidity sensor and then subjected to up to three corresponding humidity runs. Occasionally, if irreversible changes in hygroscopic material were observed as a result of water droplet impingement, the humidity sensors were replaced between these runs.

Photographs and sketches depicting typical radiosonde installation and orientation in the test section as well as the relative positions of the wind-tunnel temperature, humidity, and velocity probes are shown in Figs. 16 and 17. Figure 17 also illustrates a special dropsonde installation employing an improvised precipitation shield. Nominal test conditions and significant characteristics of the radiosonde and wind-tunnel performance for each run are summarized in Table I, Appendix II. Digitized time histories of radiosonde and test section parameters were manually traced for display in the following section as previously described.

4.2 TEST RESULTS

4.2.1 Temperature

Four dropsonde temperature-time histories are compared with spherical thermocouple probe results in Fig. 18. Good agreement was observed between each instrument in times of both slowly and rapidly varying temperature. As indicated in the test summary, these data represent only one run of a series of multiple tests conducted to evaluate deterioration of radiosonde performance with repeated and prolonged temperature variations. No such effects were detected, and the above results are representative of repeated tests.

Typical dropsonde temperature-time histories are compared in Fig. 19 with the cylindrical thermocouple probe which possessed an order of magnitude faster time response than the AMT-13 dropsonde thermistor. These results indicate that the conventional thermistor

was subject to significant time lag, manifested simply as an amplitude attenuation, only during very rapid temperature fluctuations which are not representative of expected flight conditions.

Comparisons of simultaneous dropsonde and test section measurements showed that the temperature accuracy of individual AMT-13 dropsondes may be characterized by a near uniform bias from the true value which did not deteriorate with repeated exposure. The individual biases of most of the dropsonde instruments were found distributed within 0.5°C above and below the true value, represented by the test section temperature.

Two typical rawinsonde temperature-time histories obtained consecutively are compared with the corresponding spherical thermocouple probe results in Fig. 20. The disagreement between the test section and rawinsonde measurements observed in Fig. 20a during transients is attributed to the unfavorable location of the thermocouple probes in the rawinsonde flow field. Considerably better agreement is found in Fig. 20b with the thermocouple probe located in a region of higher velocity. Nevertheless, quantitative evaluation of rawinsonde performance is restricted by spherical thermocouple probe time-response limitations.

This deficiency was overcome by utilizing the "fast response" cylindrical thermocouple probe with typical results illustrated in Fig. 21. Time-response limitations of the rawinsonde instrumentation were thus observed, appearing predominantly as amplitude attenuation during rapid fluctuation and predominantly as phase lag during slower variation. It should be pointed out again that the larger gradients were not realistic flight conditions.

The J00X-series rawinsonde temperature instrumentation was also found to be durable and reliable when subjected to repeated temperature variations. However, unlike the AMT-13 dropsonde, most of these instruments were found, by comparison with simultaneous test section measurements, to be uniformly biased above the true value by as much as 1°C.

4.2.2 Relative Humidity

Representative dropsonde humidity-time histories obtained with the standard ML-476 hygristor element are illustrated in Fig. 22. Figure 22a shows results typically found when test conditions near 100-percent RH were generated without either producing substantial water droplet contamination or without injecting liquid-nitrogen coolant.

Generally, good agreement was observed between dropsonde and wind-tunnel humidity data for quasi-steady-state relative humidity values in the range of interest above 50-percent RH. However, as expected, poorer agreement was observed during transients, in the presence of water droplet contamination, and at lower humidity levels. Humidity-time histories for test conditions employing liquid-nitrogen injection to control free-stream temperature and prevent water droplet formation are illustrated in Fig. 22b. Free-stream temperature fluctuations, accentuated by the wide difference in time-response characteristics of the CRL hygrometer and thermocouple probe, caused the apparent relative humidity fluctuations detected by the wind-tunnel instrumentation. Otherwise, no significant difference in dropsonde or wind-tunnel performance was observed for test conditions represented in Fig. 22.

Some effects of intense water droplet impingement on dropsonde performance are illustrated in Fig. 23. Generally, it was found that, on initial contact with water droplets, the dropsonde output rapidly approached 100-percent RH. With further increases in the rate of steam injection, the dropsonde instrumentation experienced an irreversible change, characterized by an inability to indicate low relative humidity levels, attributed to the removal of hygroscopic material by droplet impingement. Direct water droplet impingement is clearly indicated in Fig. 23. The relatively wide disagreement between the dropsonde and wind-tunnel measurements in the absence of droplet impingement was attributed to removal of hygroscopic material during this particular run and the preceding runs (see Test Summary Section 4.1).

A sample relative humidity-time history, obtained with a non-standard "CM" hygristor element shown in Fig. 24, illustrates the general similarity of results found for dropsondes employing each type hygristor.

Humidity test results from a dropsonde incorporating an improvised precipitation shield to minimize water droplet impingement are compared with the wind-tunnel instrumentation results in Fig. 25. An unshielded dropsonde and the tunnel instrumentation responded to water droplet impingement as shown in Fig. 25a in the manner previously described. Significantly, however, the shielded dropsonde was found to track the CRL hygrometer closely in the presence of water droplet impingement, indicating that both the shielded dropsonde and the CRL hygrometer were responding only to the relative humidity of the air-water vapor mixture. An examination of shielded and unshielded dropsonde results of the end of the run in Fig. 25a, where steam injection was completely terminated, clearly illustrates the grossly erroneous

17

indication at lower relative humidity levels caused by removal of hygroscopic material. Humidity test results obtained without droplet impingement from a shielded and unshielded dropsonde (at a nominal free-stream velocity of 15 ft/sec) are illustrated in Fig. 25b for comparison with rawinsonde test results under identical conditions. Excellent agreement between the dropsonde and tunnel instrumentation outputs was noted over the entire relative humidity range.

Representative rawinsonde humidity-time histories obtained during two separate wind-tunnel entries are presented in Fig. 26. Data in Fig. 26a, obtained during the initial test entry, were evaluated using the baseline environmental chamber provided with the rawinsondes for calibrating hygristor elements. Relatively good agreement was obtained with the CRL hygrometer output at high relative humidity levels. The poorer agreement at lower levels only was attributed to defective baseline equipment since rawinsonde indications at high humidity levels were insensitive to errors in baseline humidity. Data in Fig. 26b, obtained during the second entry, were evaluated using wind-tunnel conditions of approximately 33-percent RH to calibrate the humidity elements. A significant improvement in agreement between rawinsonde and wind-tunnel results was thereby observed over the entire range of relative humidity.

SECTION V
CONCLUDING REMARKS

Some significant results of these environmental tests are itemized below:

1. Excellent test section flow quality, characterized by temperature and relative humidity uniformity well within ±0.25°C and ±1.5 percent, respectively, was found under all operating conditions, thus making the facility ideally suited for meteorological testing.

2. Quasi-steady dropsonde and rawinsonde temperature measurements were found to have been extremely accurate, often within the ±0.25°C total uncertainty of the wind-tunnel standard.

3. Dropsonde and rawinsonde humidity instrumentation also yielded generally satisfactory results except under the influence of intense water droplet impingement.

4. Improvised precipitation shields fitted over dropsonde humidity elements eliminated water droplet impingement and permitted measurement of the mixture relative humidity.

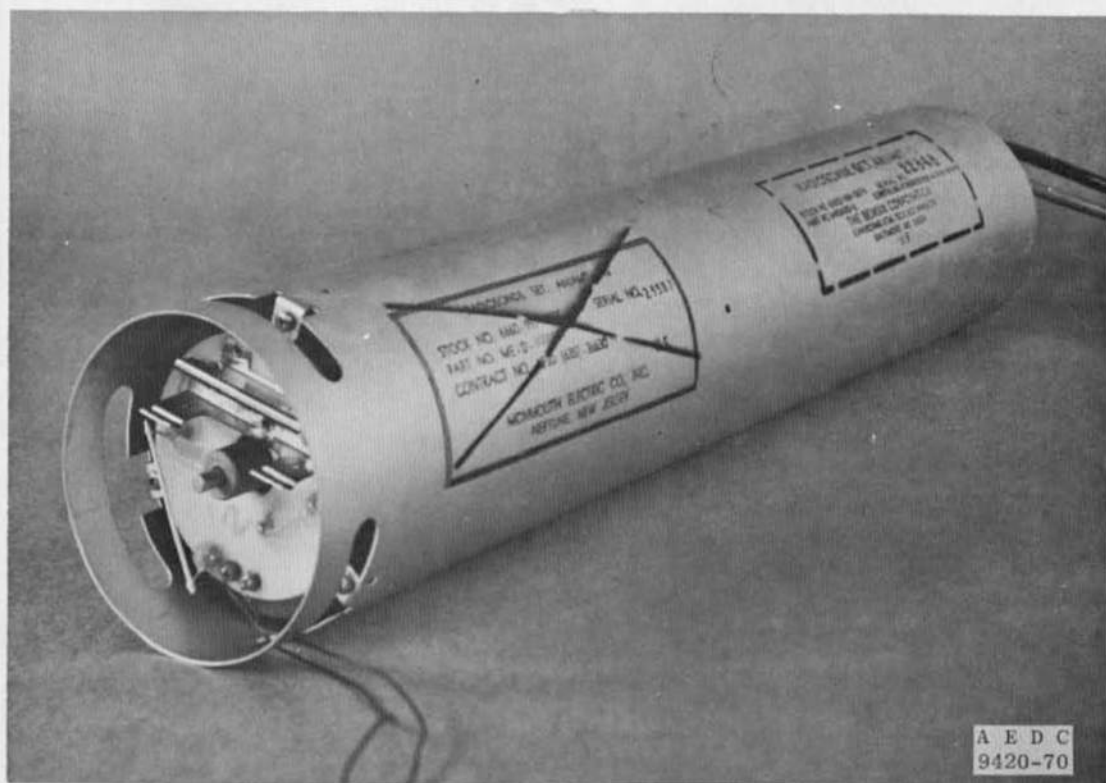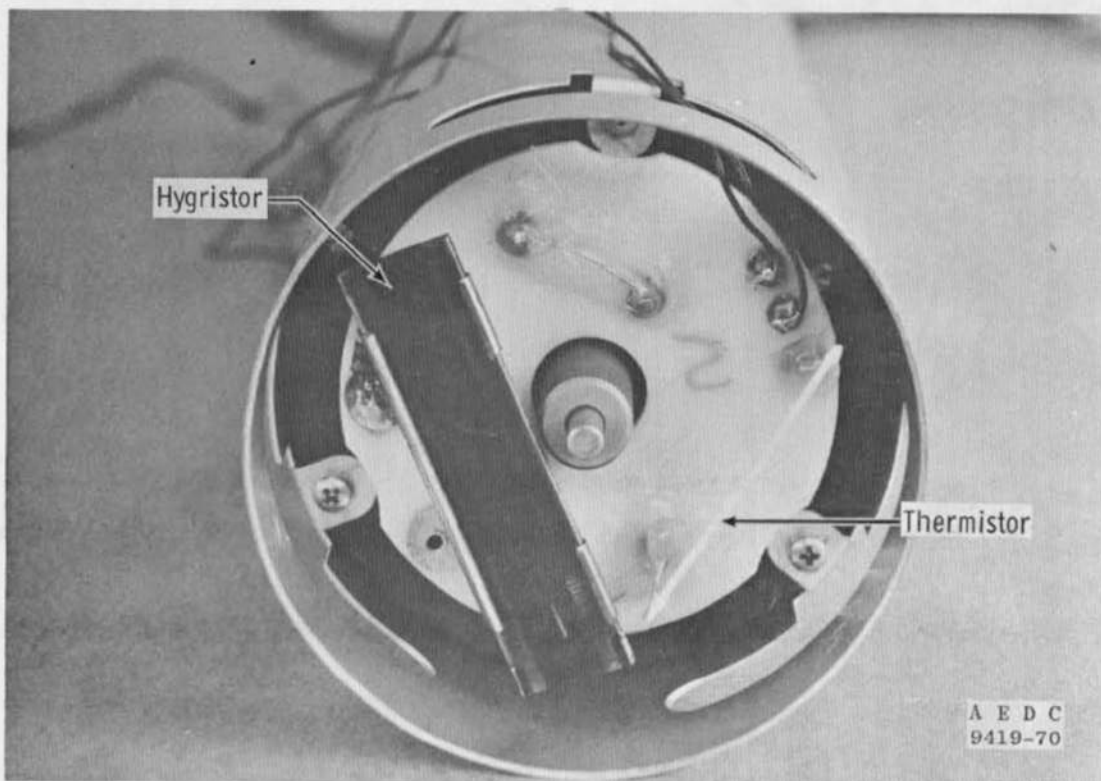**APPENDIXES**
I. ILLUSTRATIONS
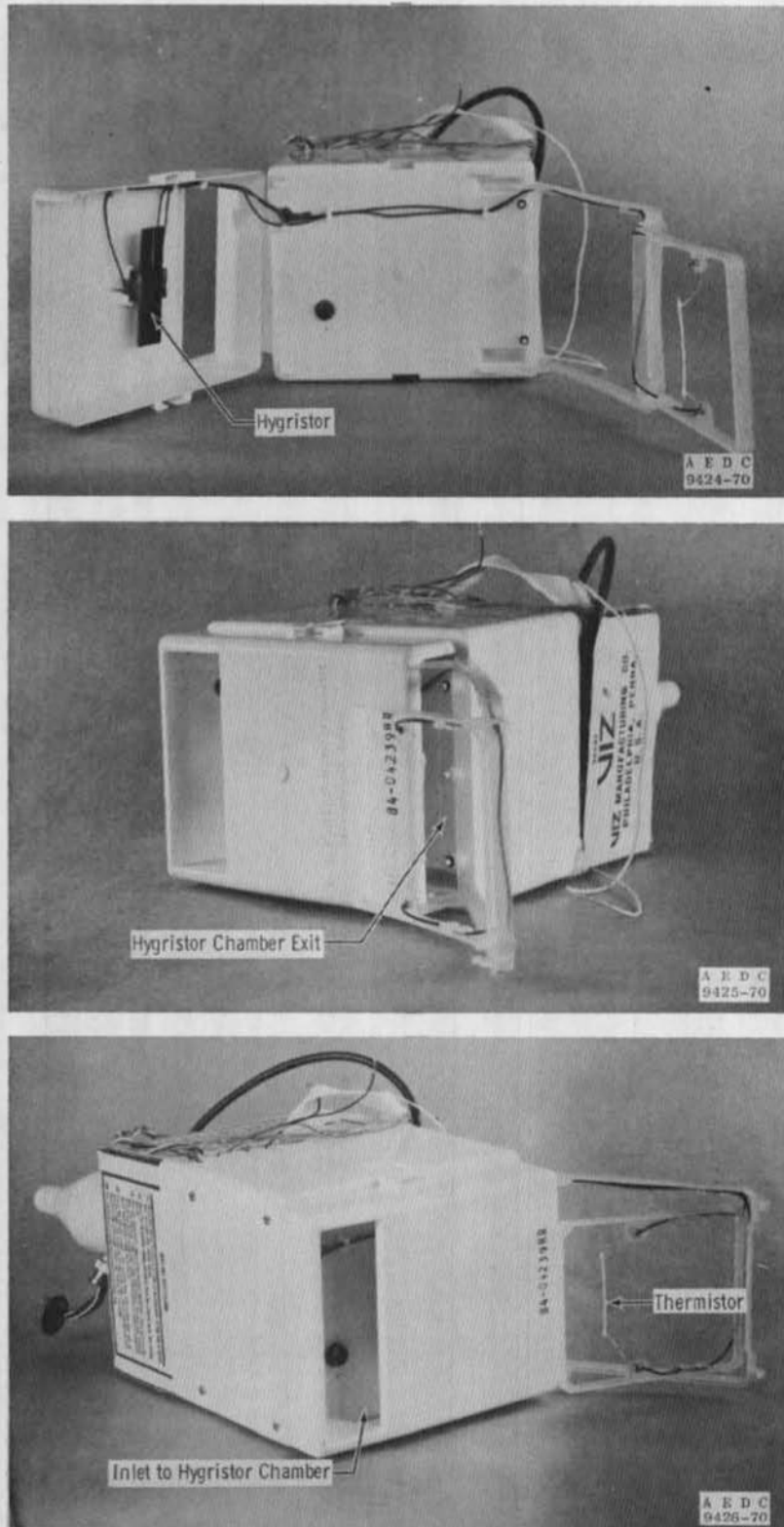II. TABLES

Fig. 1 AMT-13 Dropsonde Photographs

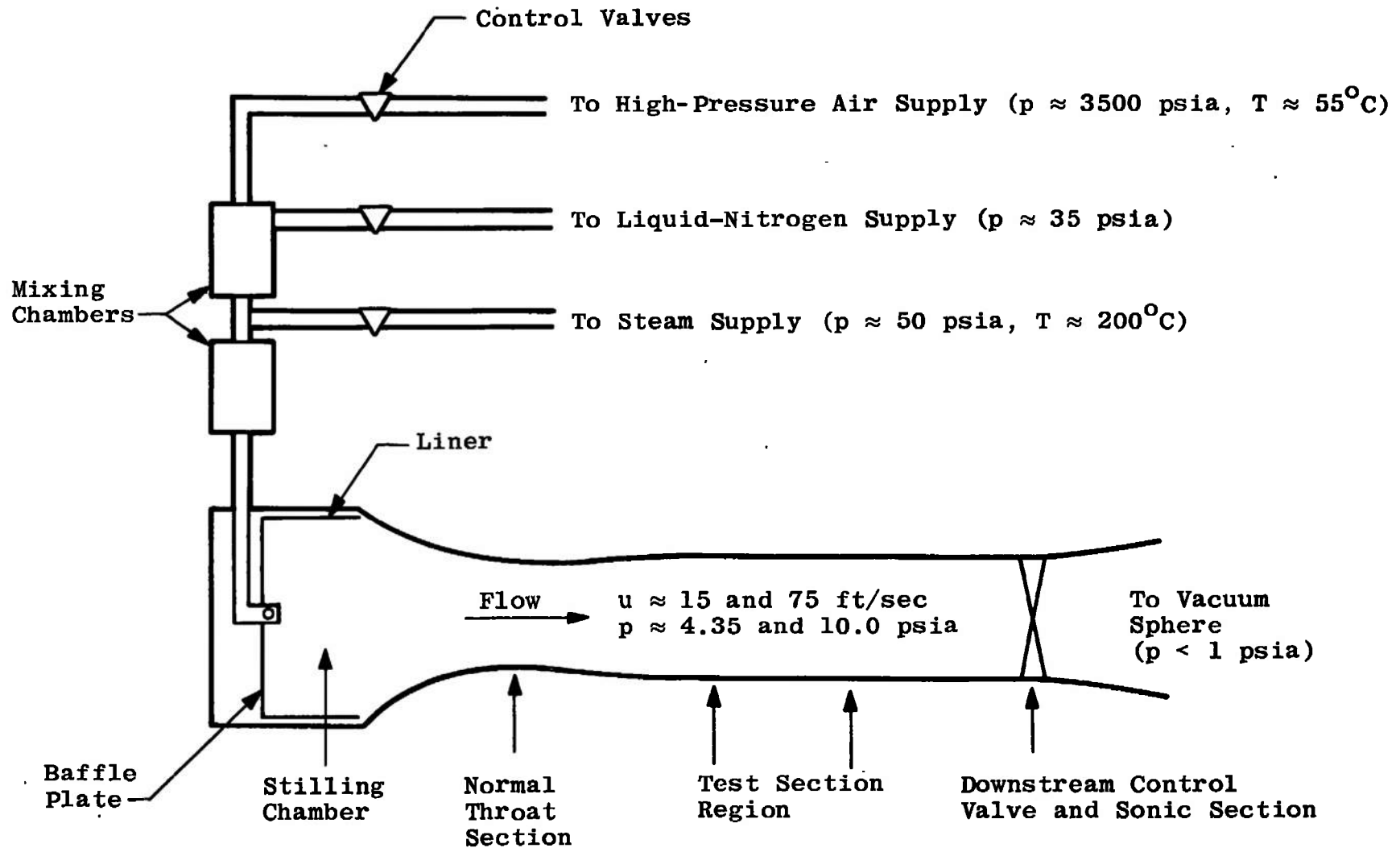Fig. 2 J00X-Series Rawinsonde Photographs

Control Valves

To High-Pressure Air Supply (p $\approx$ 3500 psia, T $\approx$ 55°C)

To Liquid-Nitrogen Supply (p $\approx$ 35 psia)

Mixing
Chambers

To Steam Supply (p $\approx$ 50 psia, T $\approx$ 200°C)

Liner

Flow   u $\approx$ 15 and 75 ft/sec
p $\approx$ 4.35 and 10.0 psia

To Vacuum
Sphere
(p < 1 psia)

Baffle
Plate

Stilling
Chamber

Normal
Throat
Section

Test Section
Region

Downstream Control
Valve and Sonic Section

Fig. 3 Test Facility Schematic Drawing
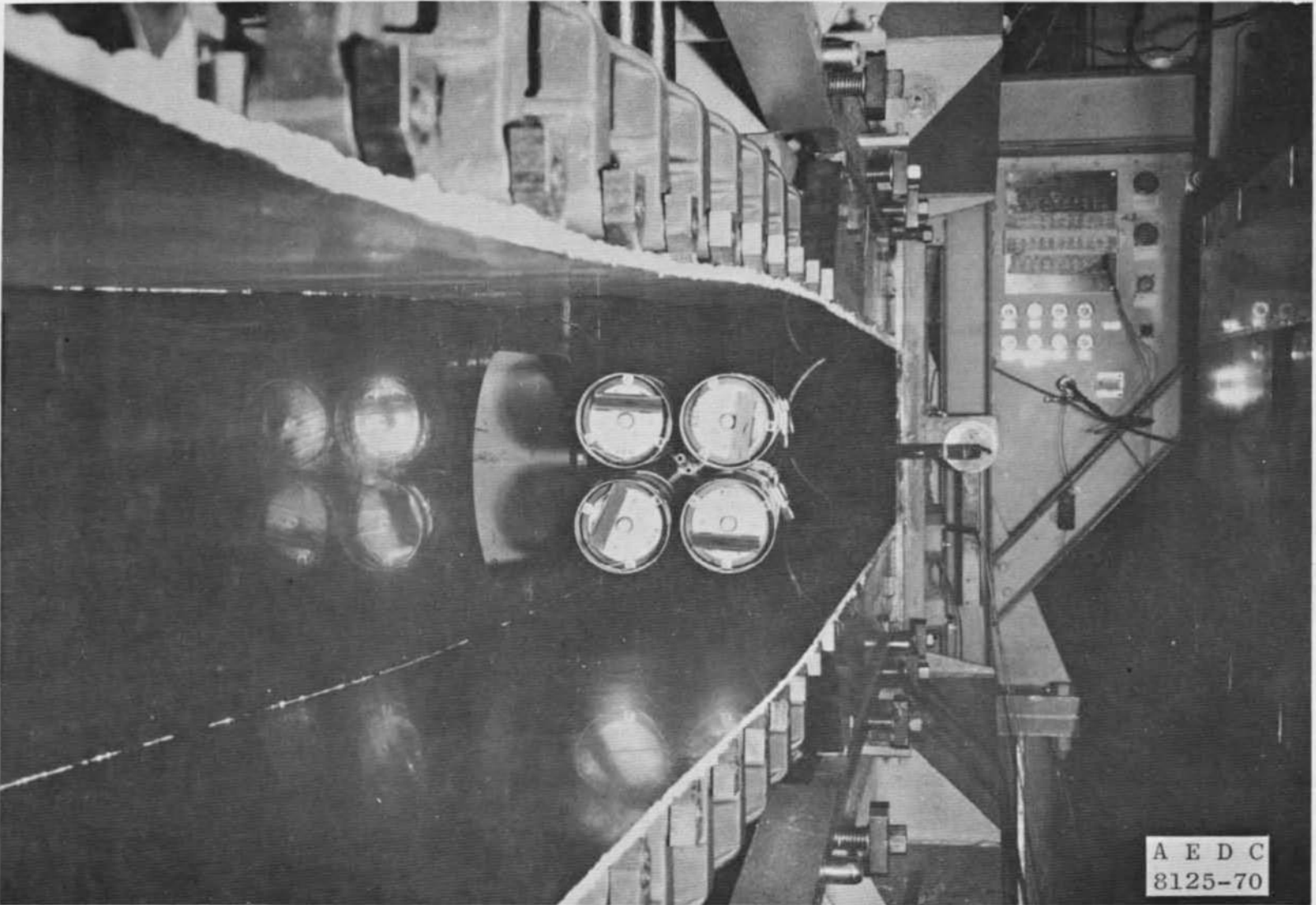
Fig. 4   Test Section Photograph with Dropsondes Installed
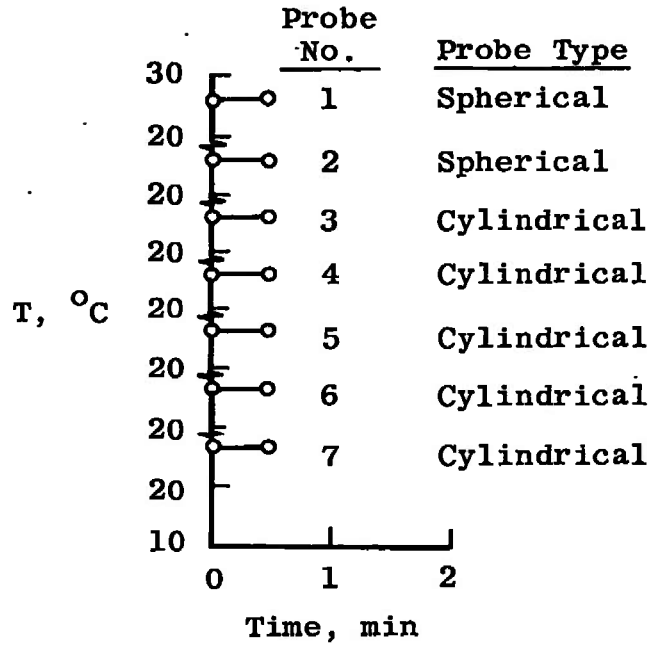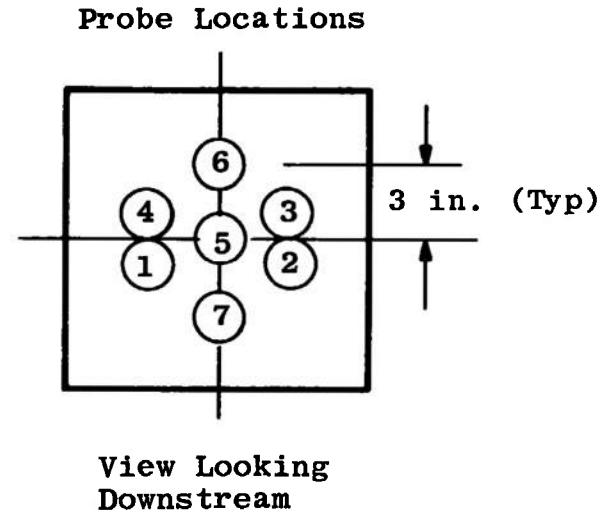
Fig. 5 Thermocouple Probe Calibration
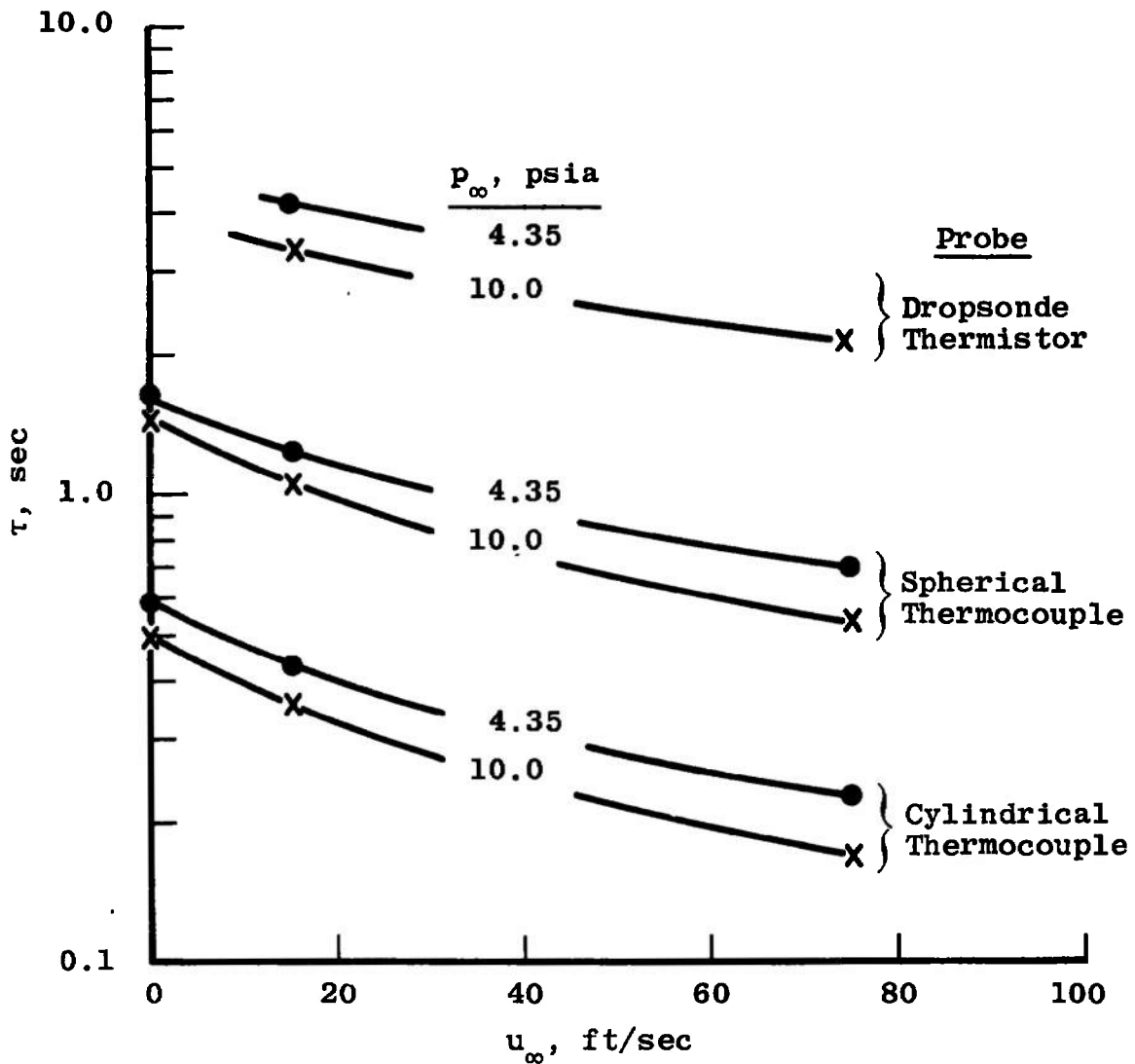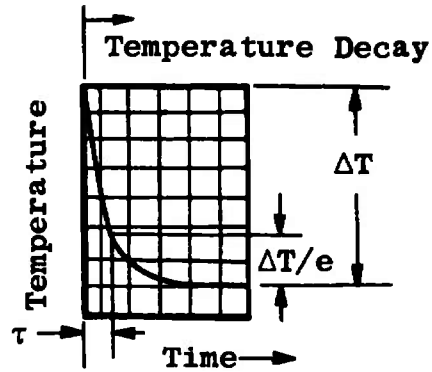
Fig. 6 Temperature Probe Time-Response Characteristics
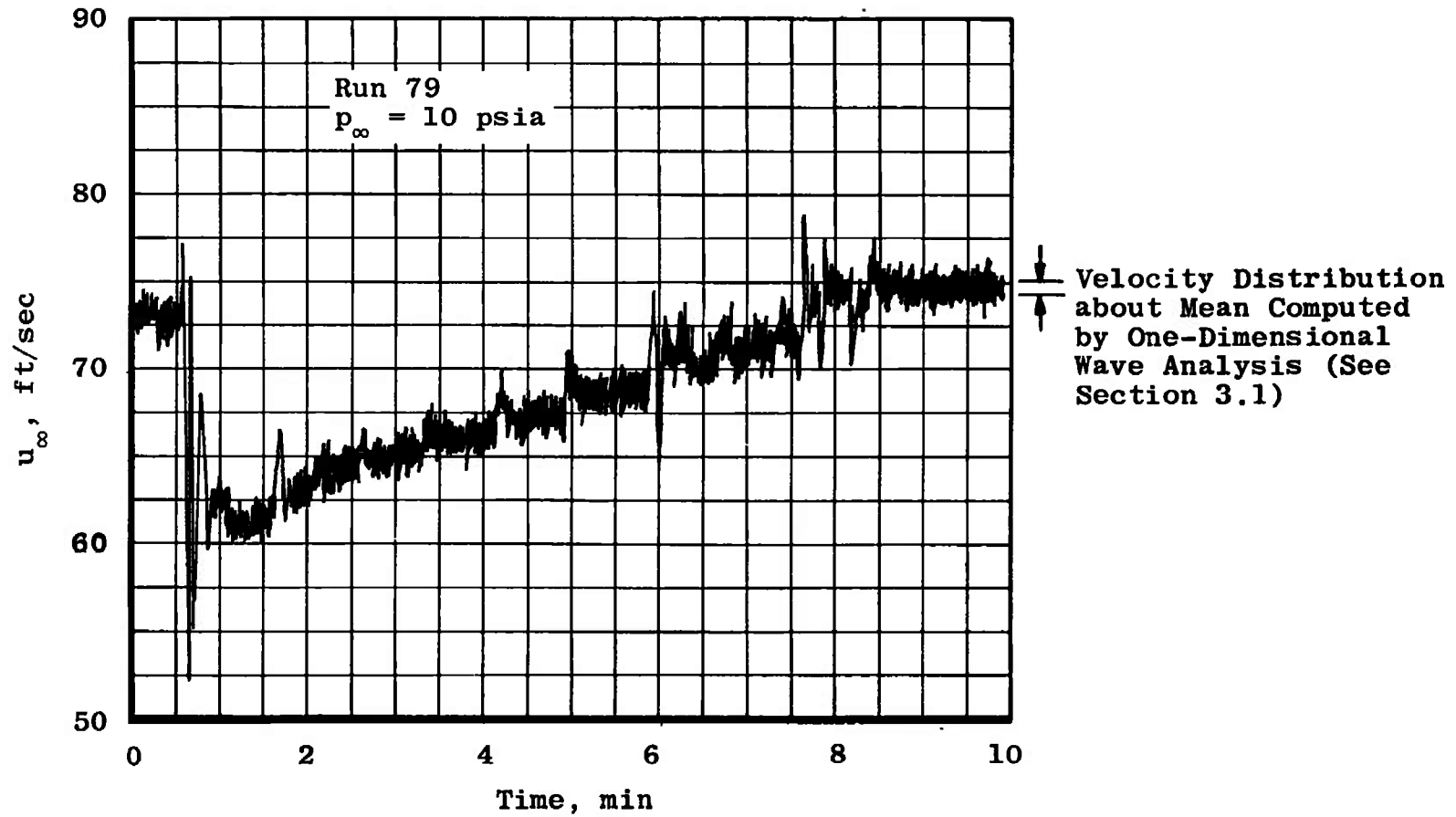
a. Liquid-Nitrogen Injection
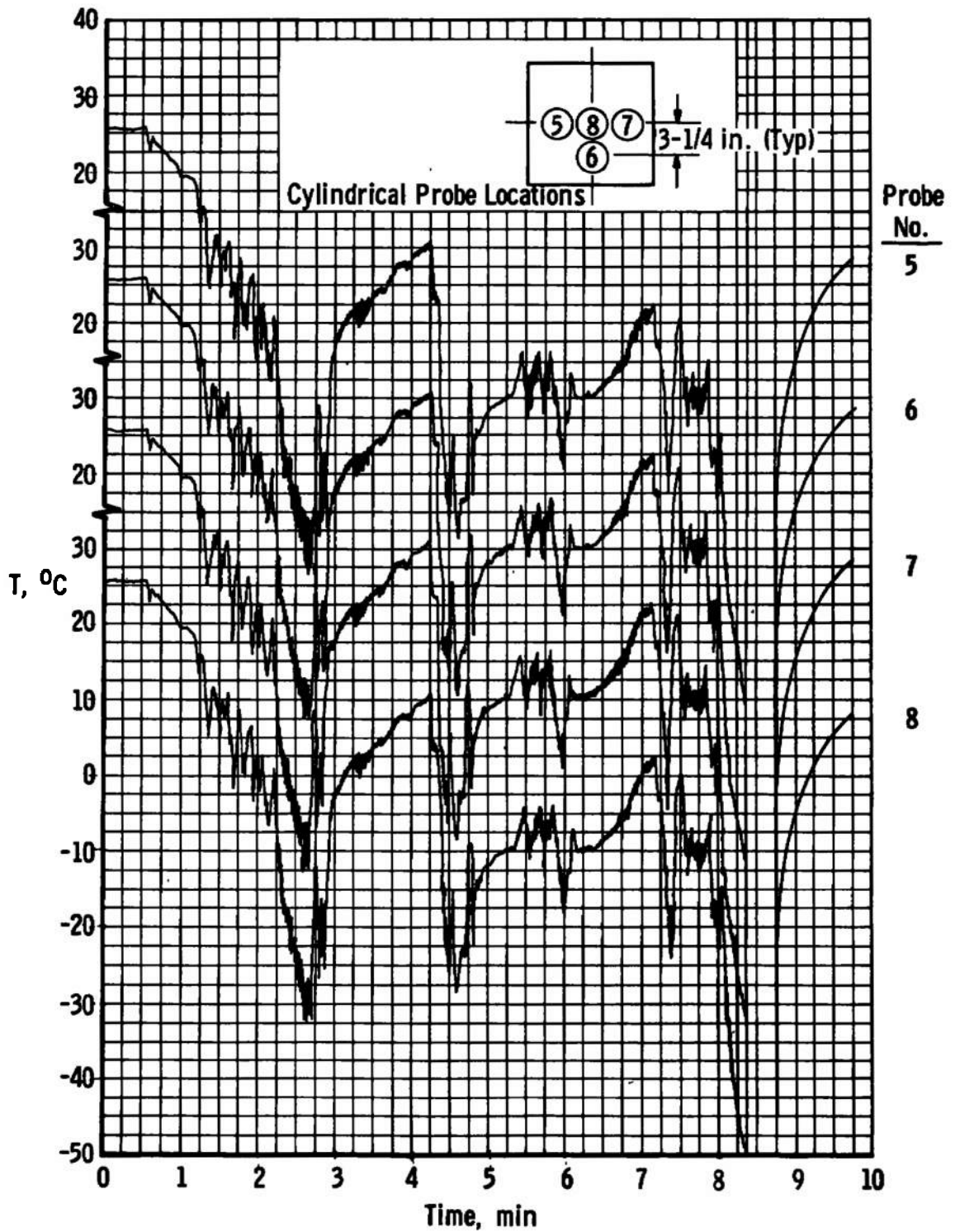Fig. 7 Typical Free-Stream Velocity Characteristics
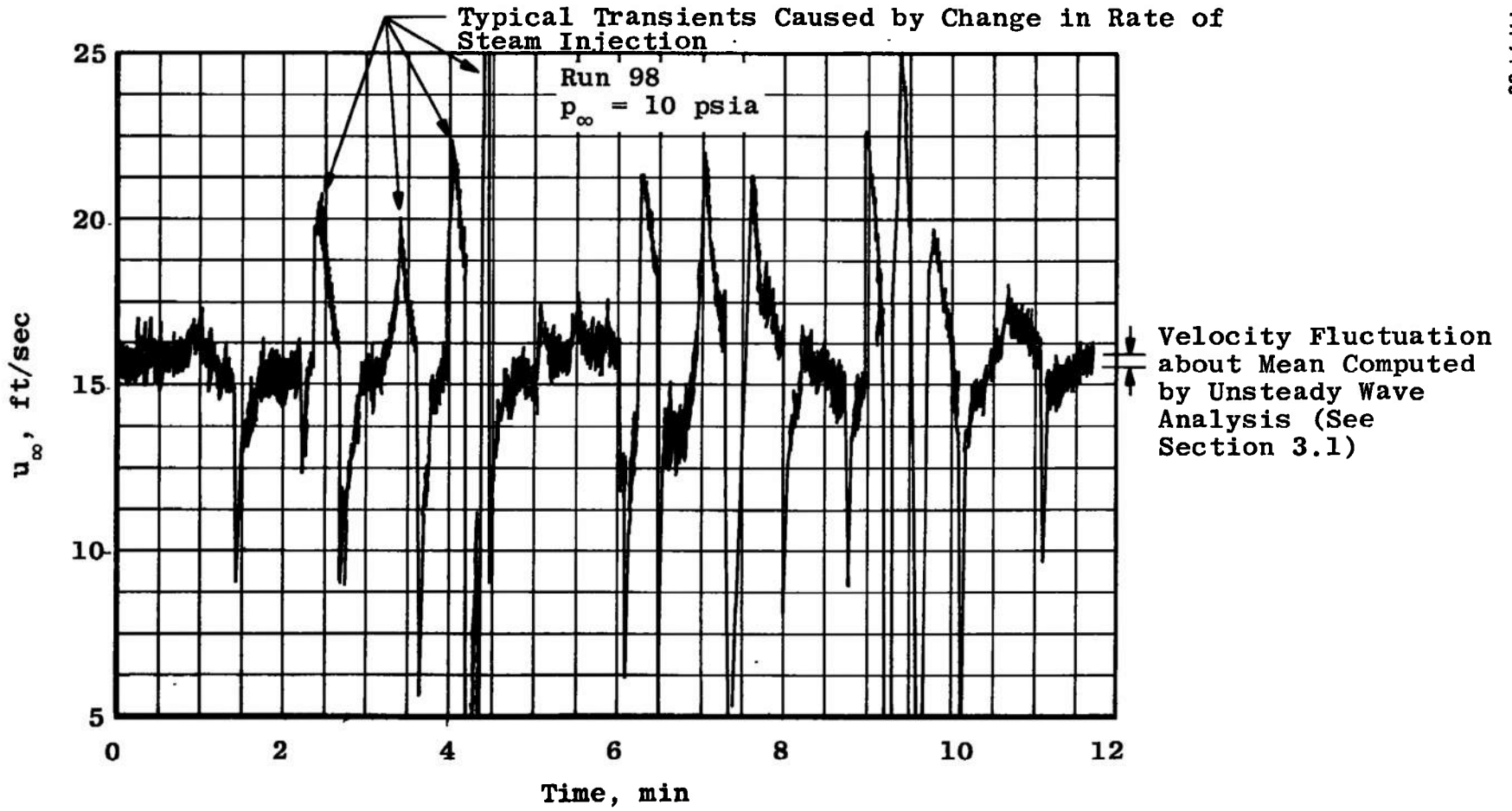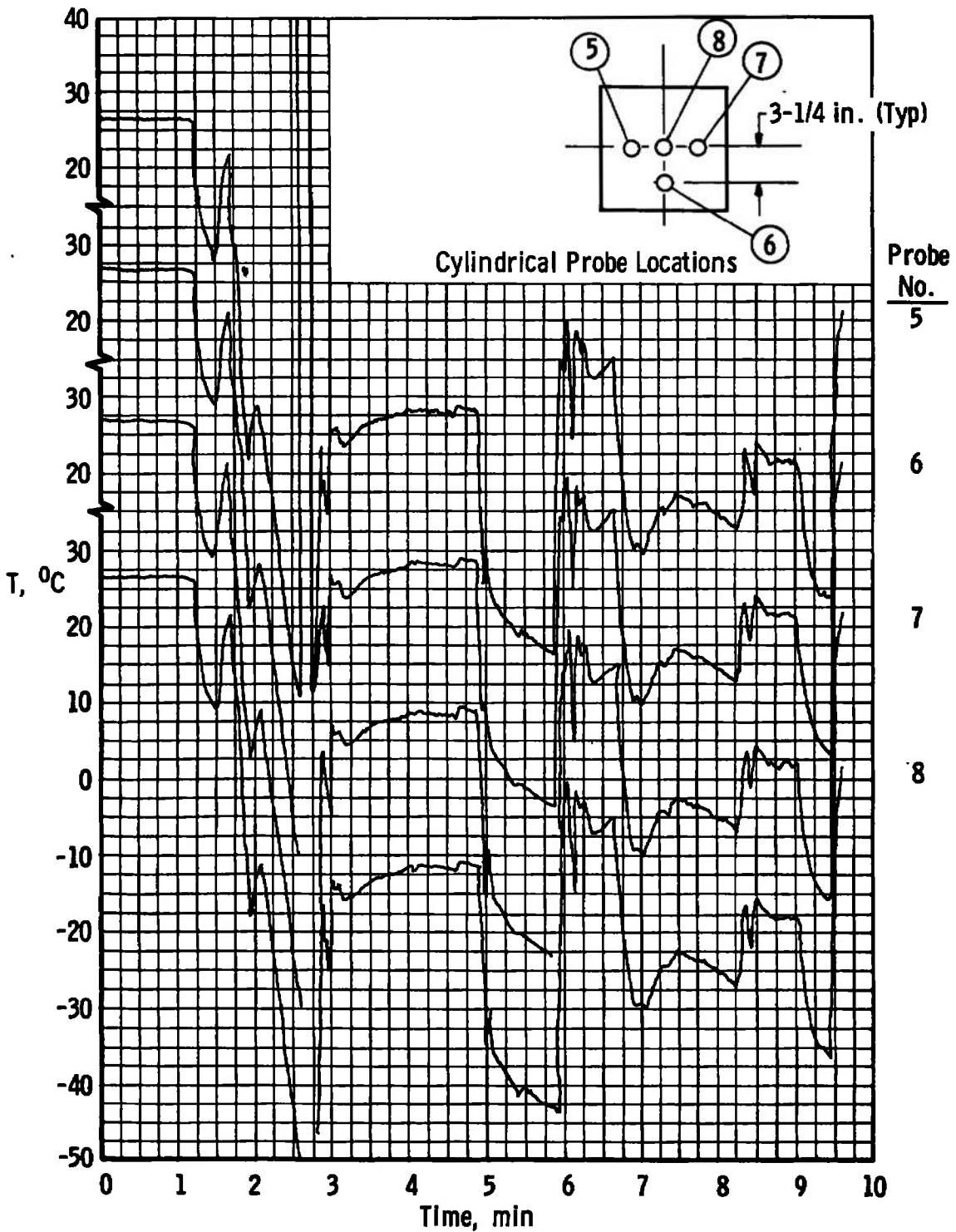
b. Steam Injection
Fig. 7 Concluded
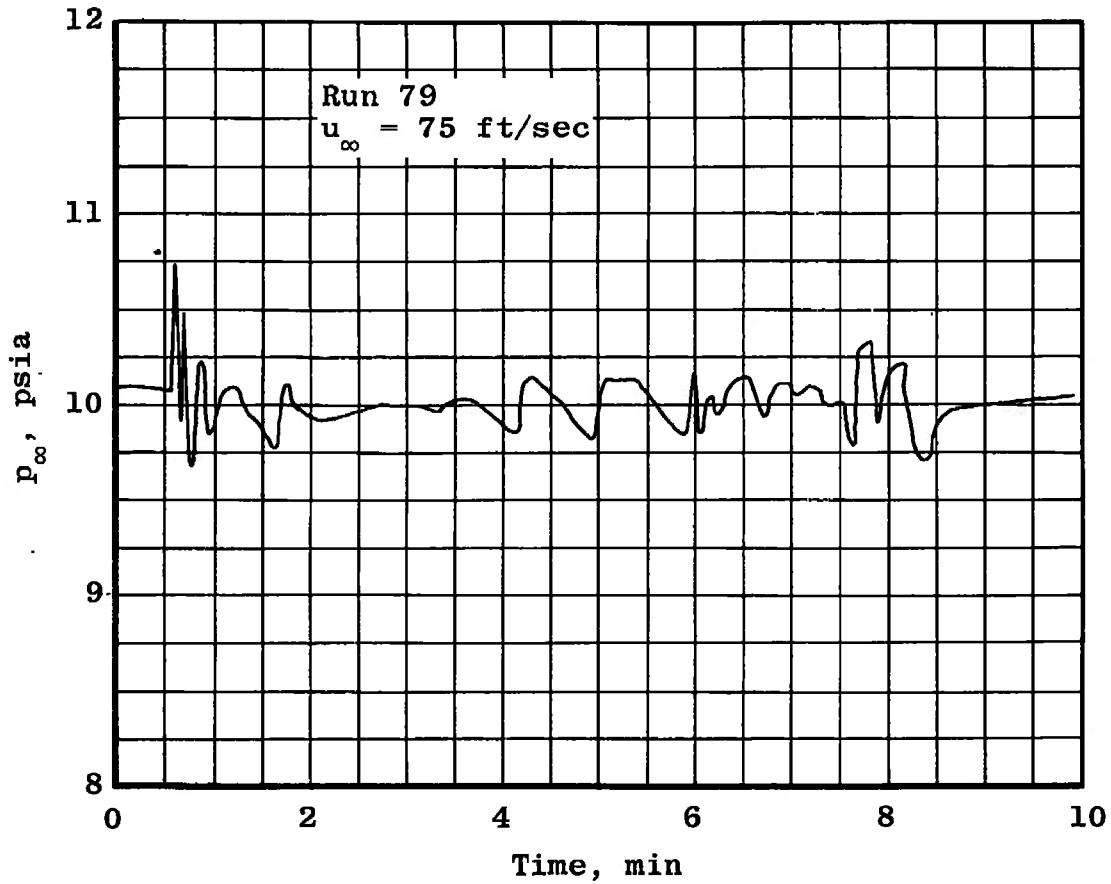
a. Liquid-Nitrogen Injection
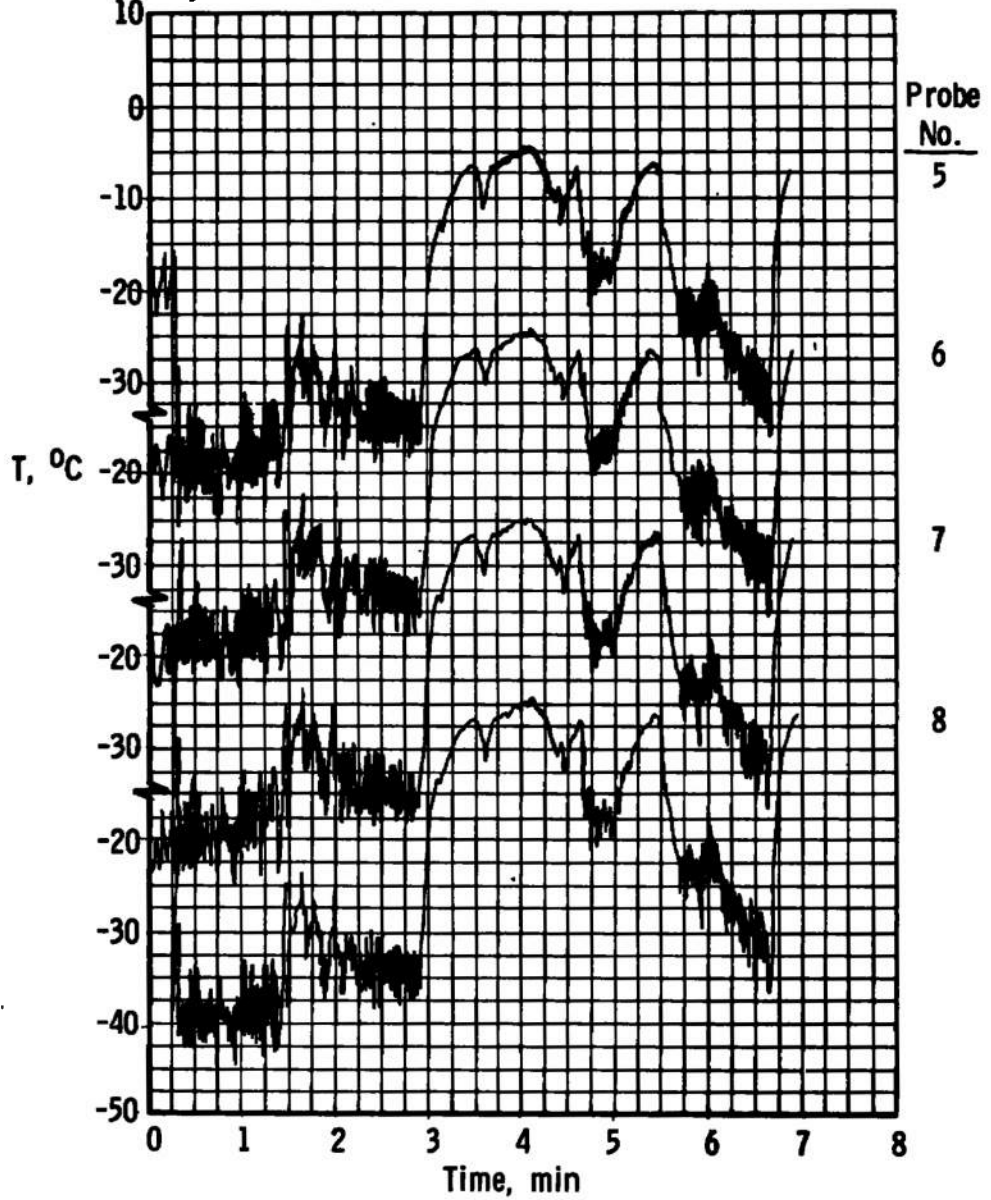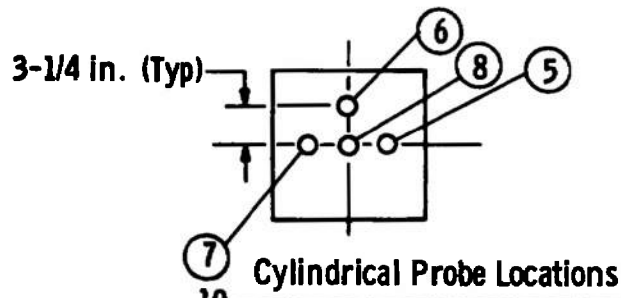Fig. 8 Typical Free-Stream Pressure Characteristics
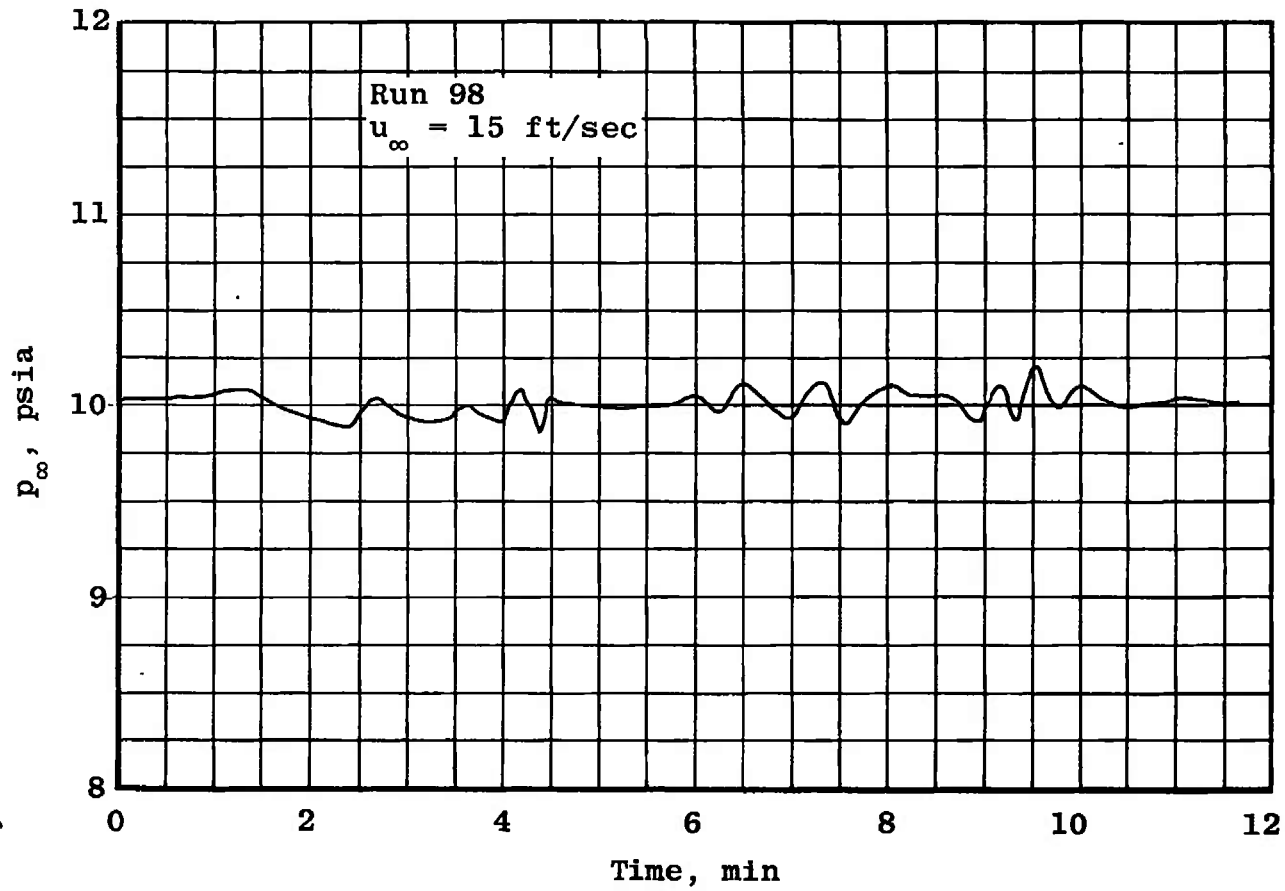
b. Steam Injection
Fig. 8 Concluded

a. u_∞ = 75 ft/sec, p_∞ = 4.35 psia, Rake Orientation 1
Fig. 9 Free-Stream Temperature Uniformity Measurements

b. u_∞ = 75 ft/sec, p_∞ = 10.0 psia, Rake Orientation 1
Fig. 9 Continued

3-1/4 in. (Typ)

Cylindrical Probe Locations

c. u_∞ = 75 ft/sec, p_∞ = 4.35 psia, Rake Orientation 2
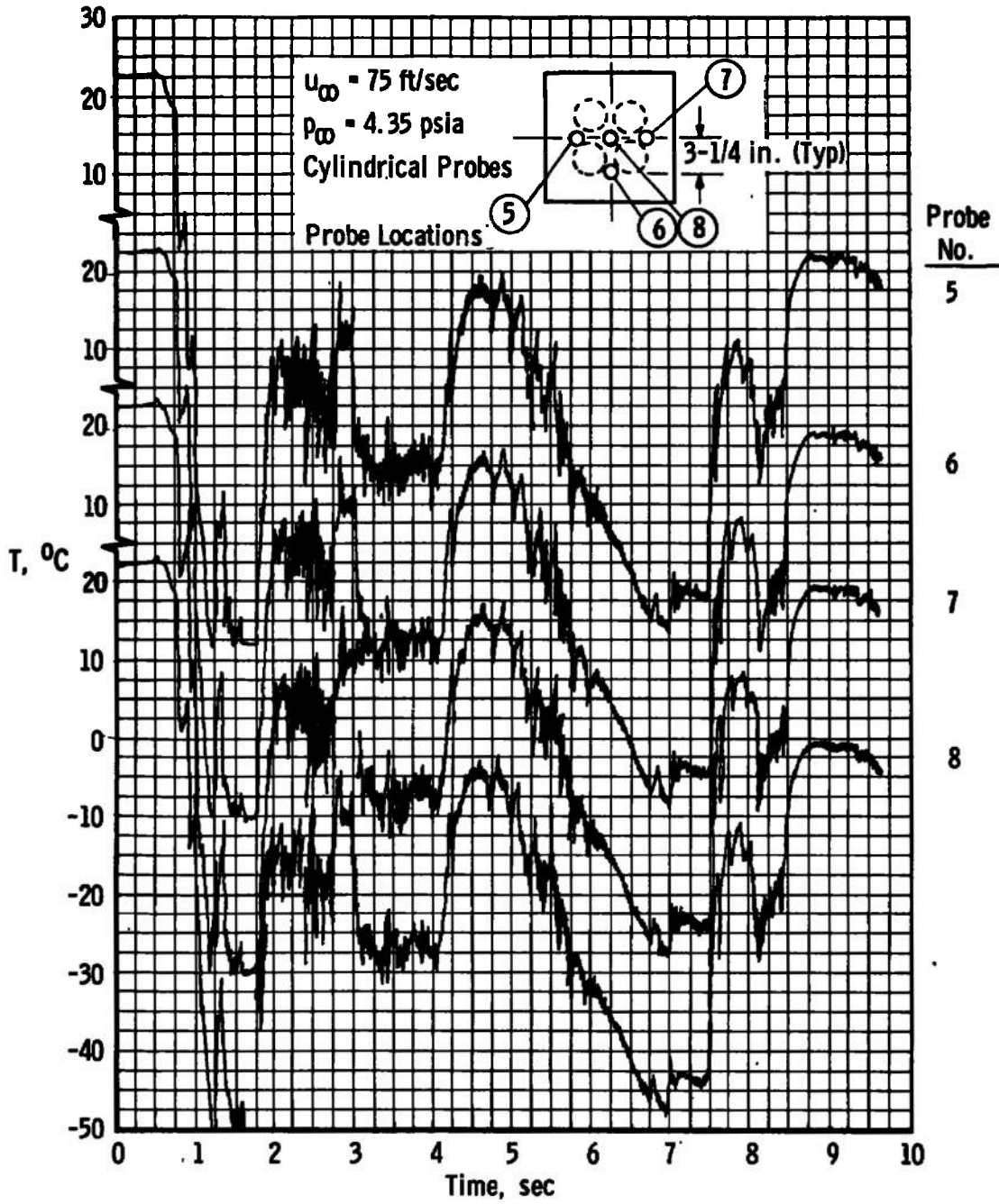Fig. 9 Concluded

33

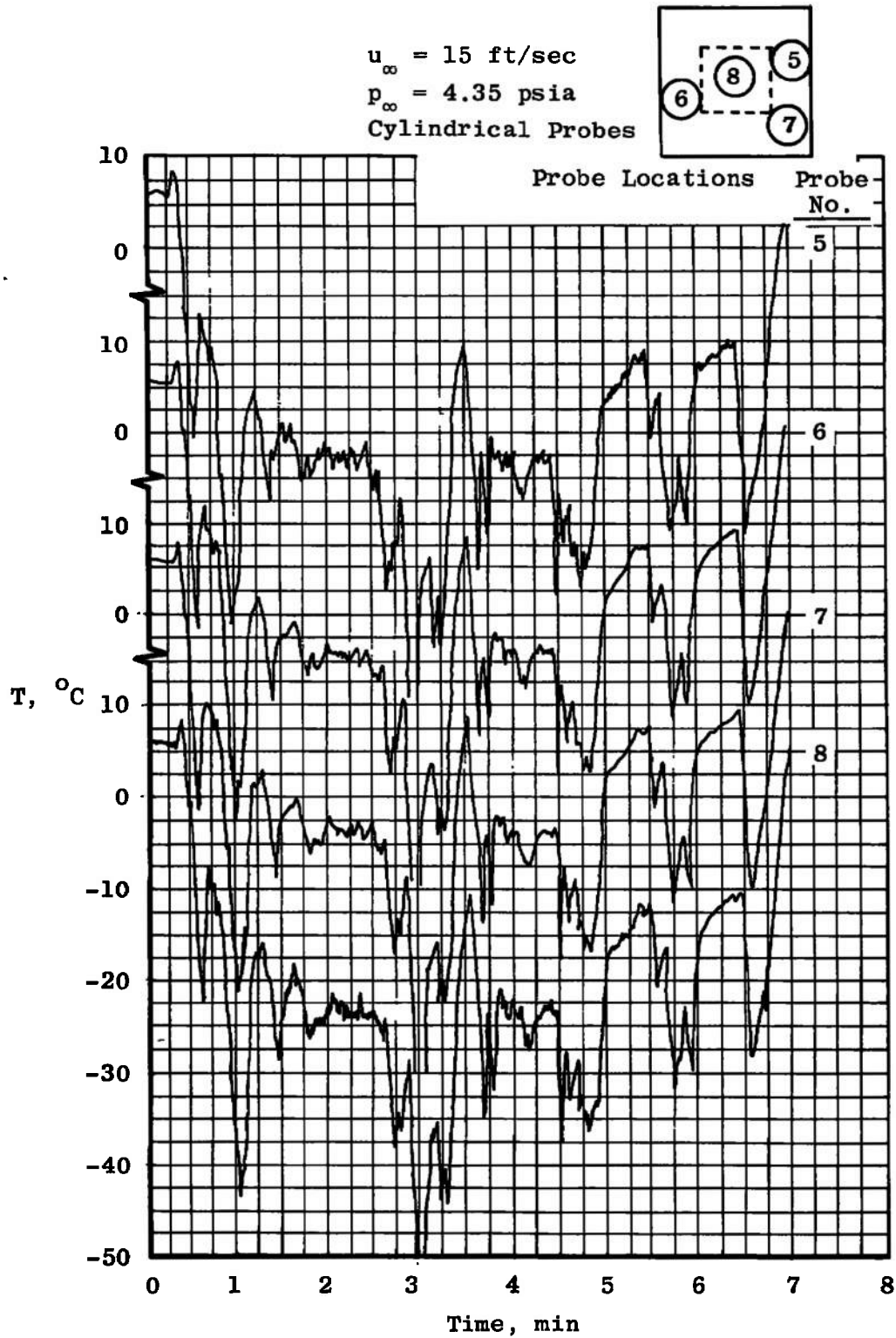Fig. 10 Free-Stream Temperature Uniformity Measurements, Dropsondes Installed

Fig. 11 Free-Stream Temperature Uniformity Measurements, Rawinsonde Installed
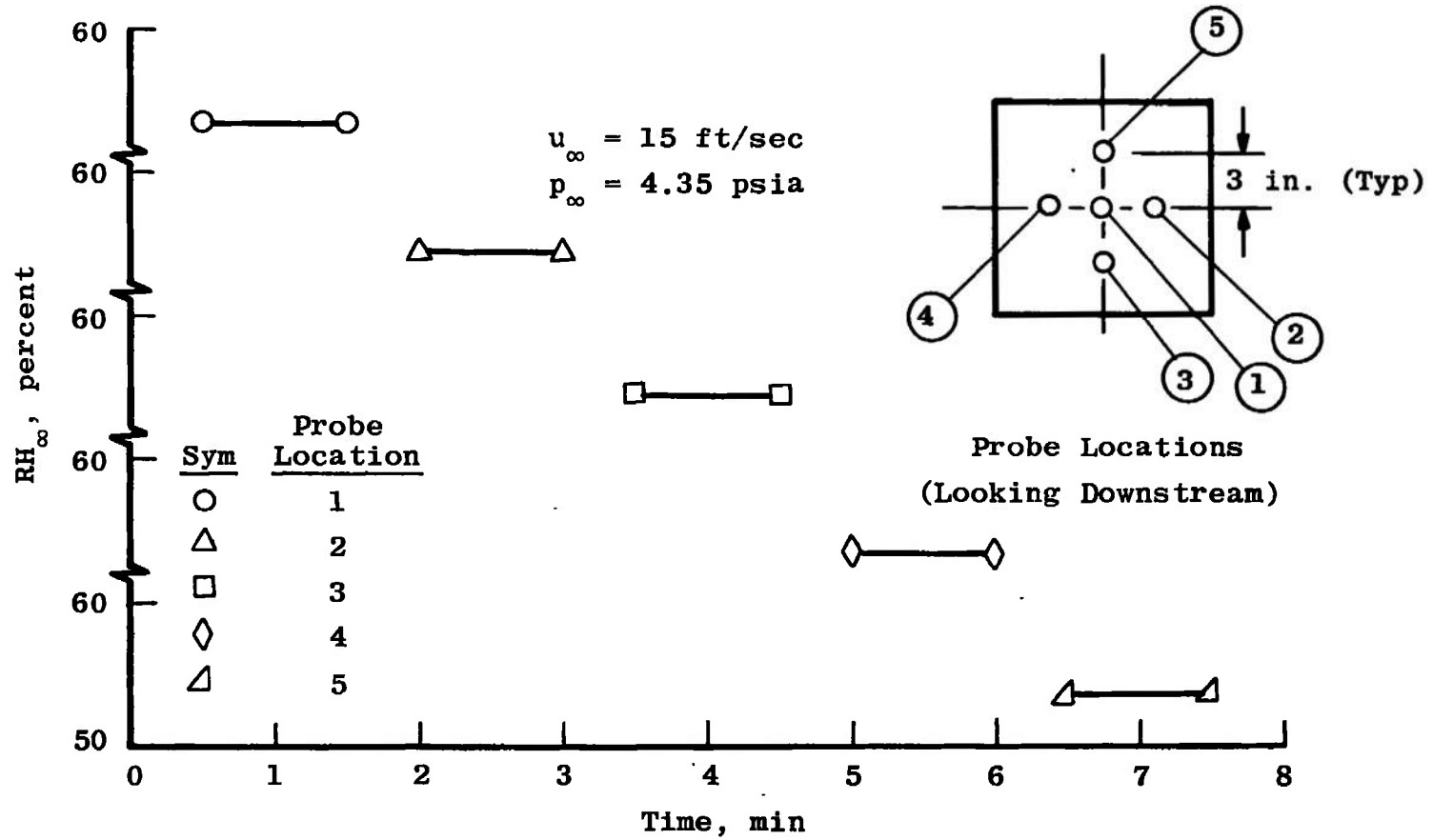
Fig. 12 Steady-State Free-Stream Relative Humidity Uniformity Measurements
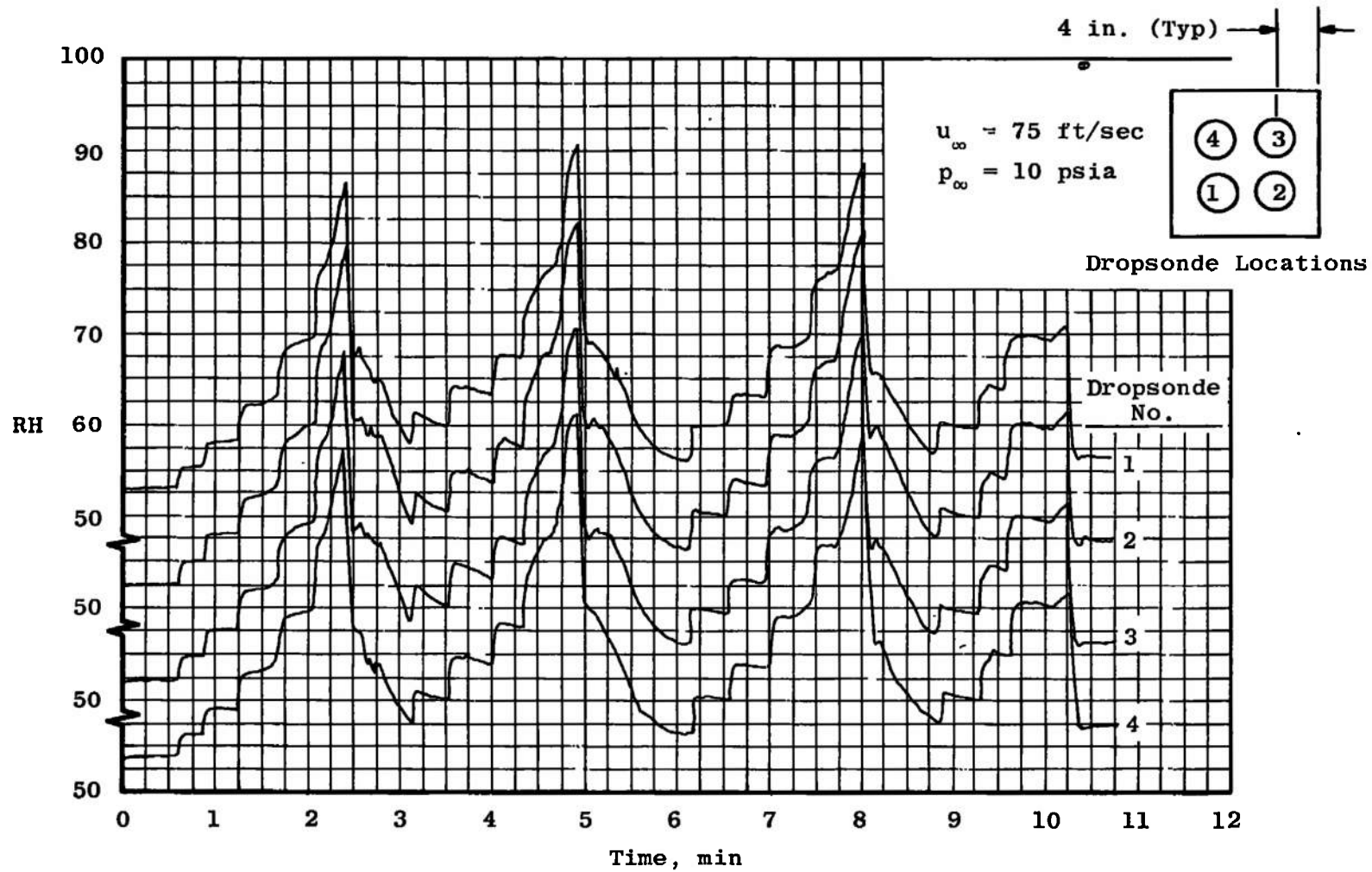
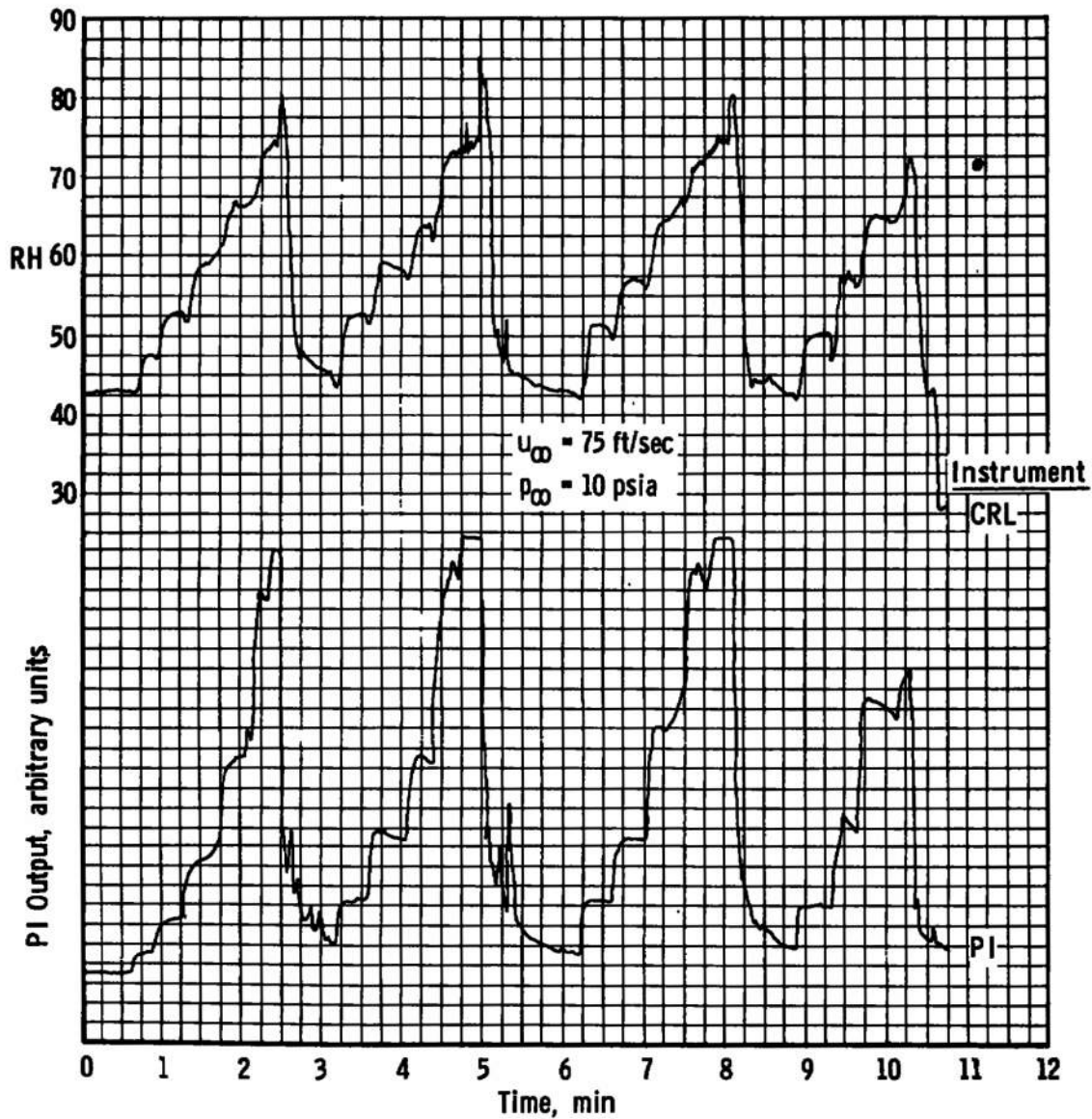Fig. 13 Time-Dependent Free-Stream Relative Humidity Uniformity Measurements

Fig. 14 Response of Wind-Tunnel Relative Humidity Instrumentation to Normal Humidity Variation
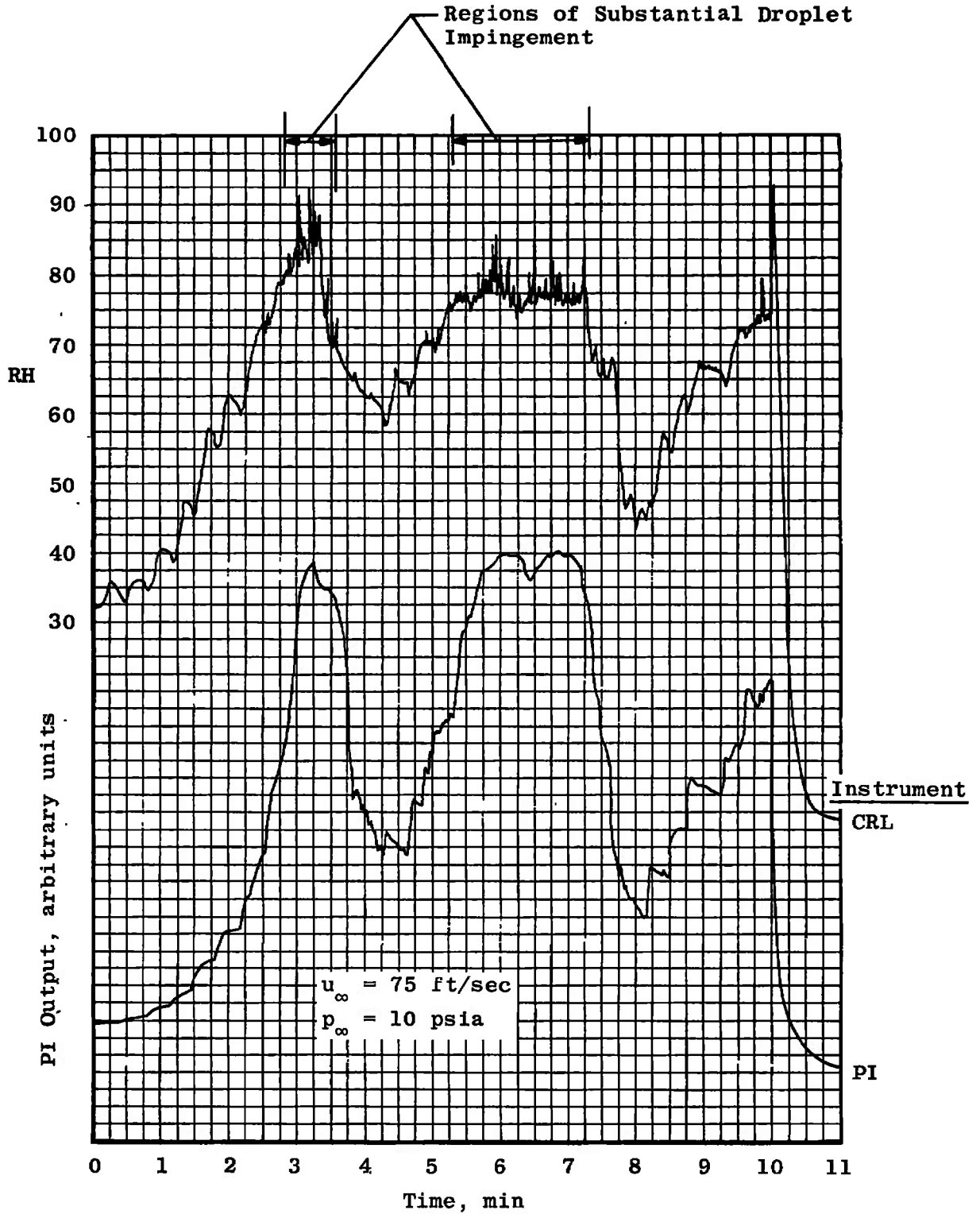
Fig. 15 Effects of Water Droplet Impingement on Performance of Wind-Tunnel Relative Humidity Instrumentation

Fig. 16 Radiosonde Installation Photographs

4 in.

←4 in. (Typ)→

3 4 — **3-1/2 in.**

2 1

Numerals Denote
Dropsonde Location

**Standard Dropsonde
Installation**

←12 in.→

2 1

**Shielded Dropsonde
Installation**

Top View

u_∞

1 in.

Thermistor

4-1/2 in.— **←6 in.→**

2-1/2 in.

Rawinsonde Installation
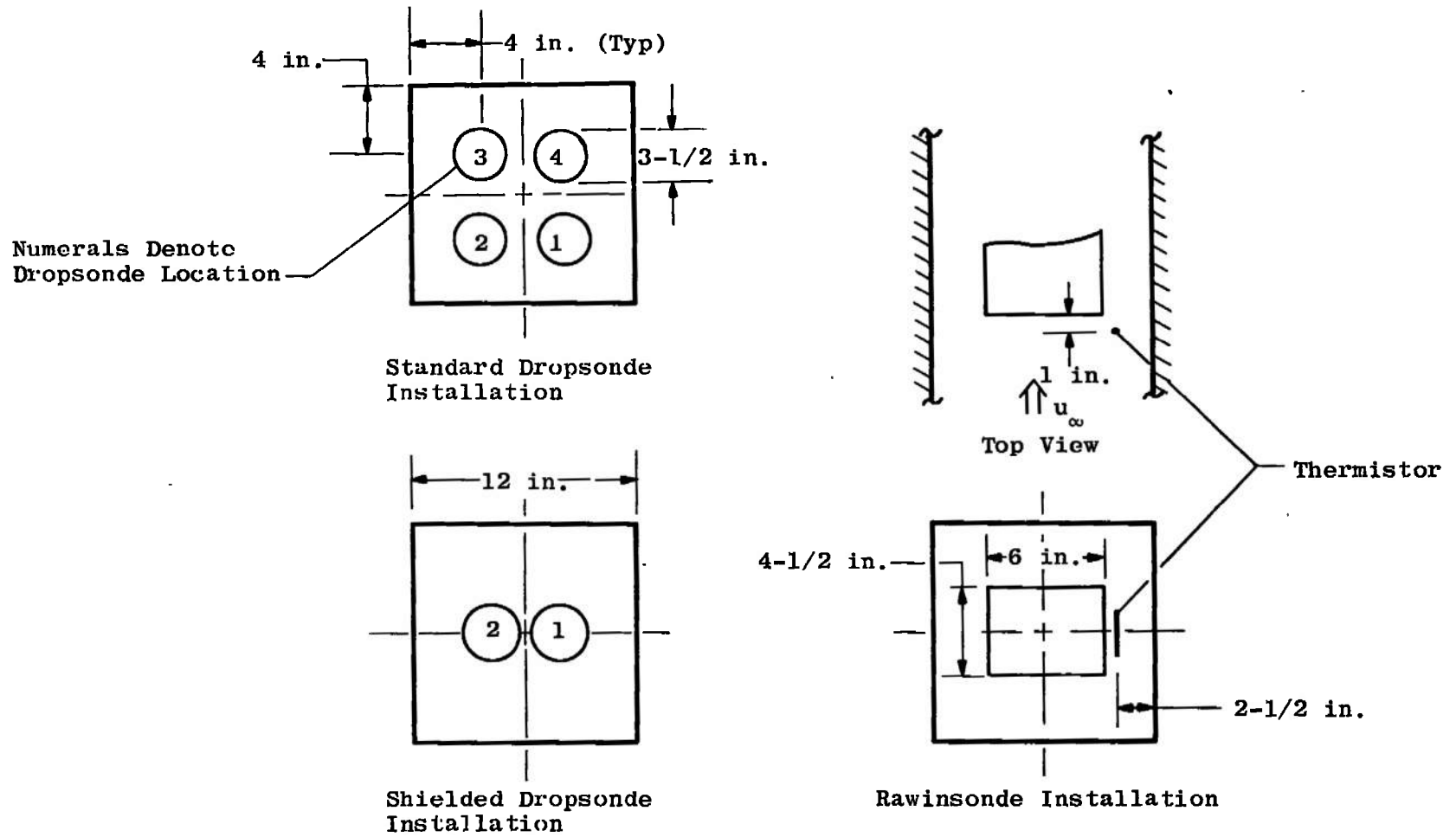
Notes: Views Looking Downstream Unless Noted
         All Dimensions in Inches

Fig. 17 Radiosonde Installation Sketches

Fig. 18 Comparison of Dropsonde and Spherical Thermocouple Reference Probe Temperature Results
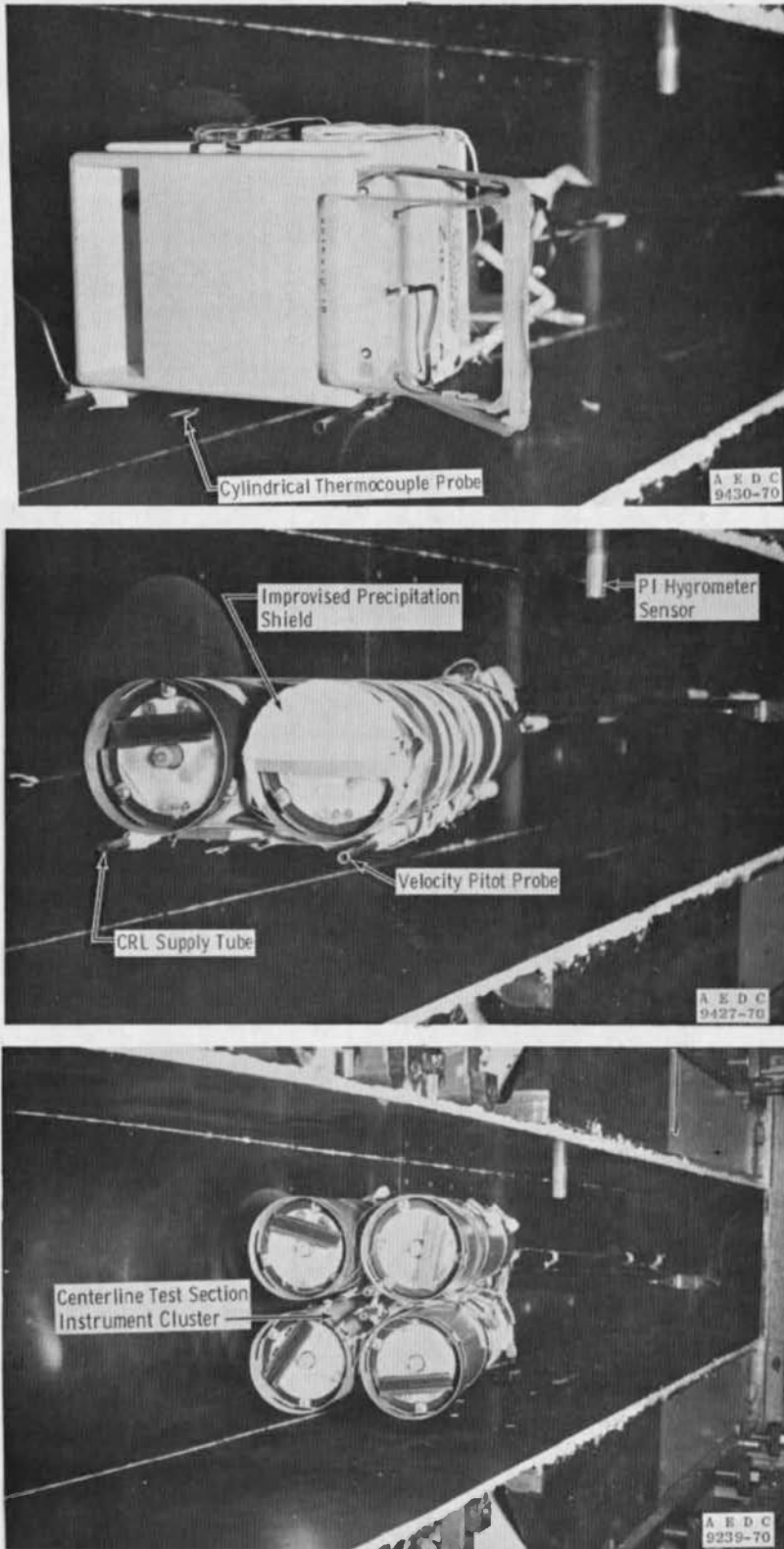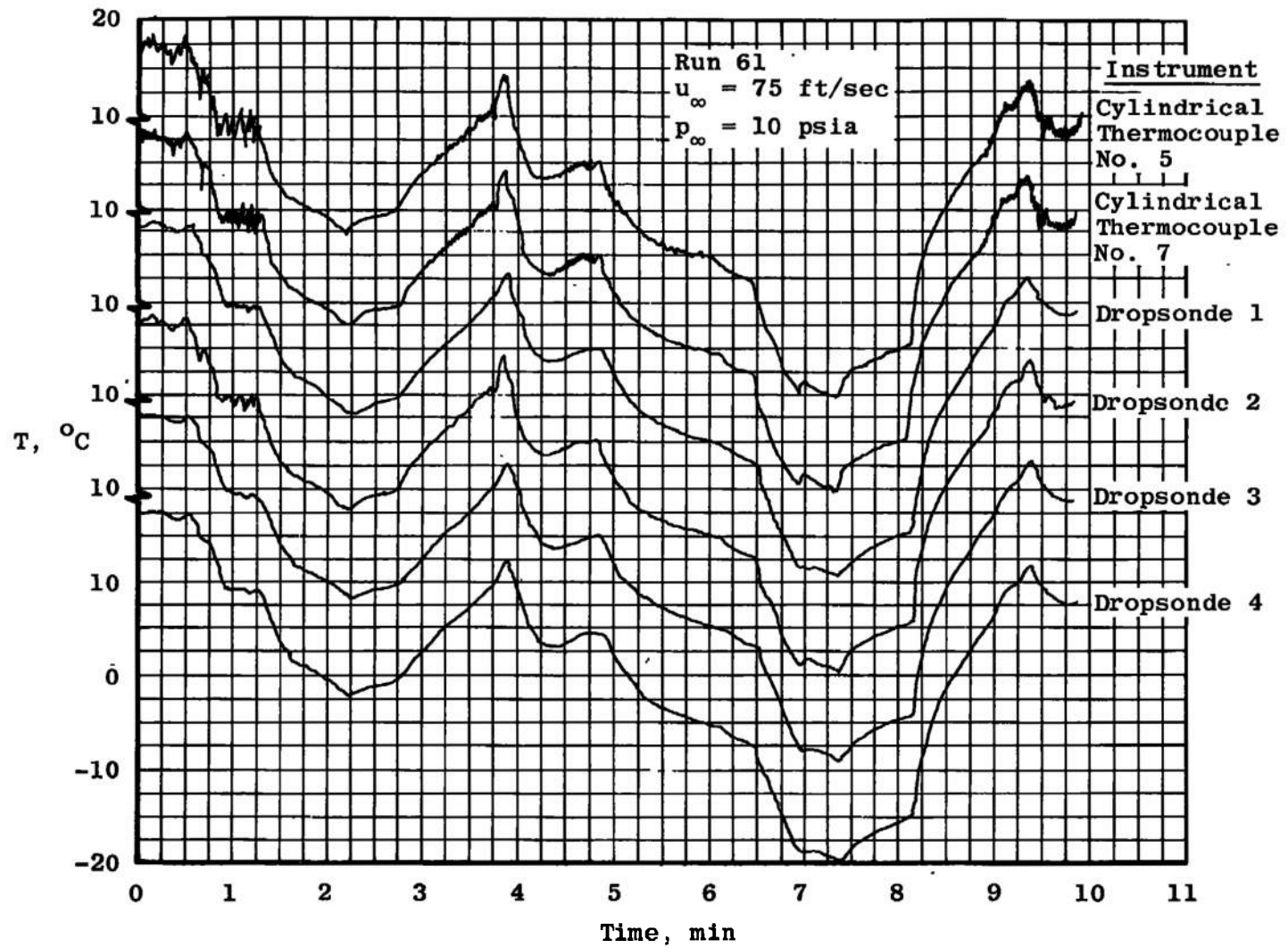
Fig. 19 Comparison of Dropsonde and Cylindrical Thermocouple Reference Probe Temperature Results
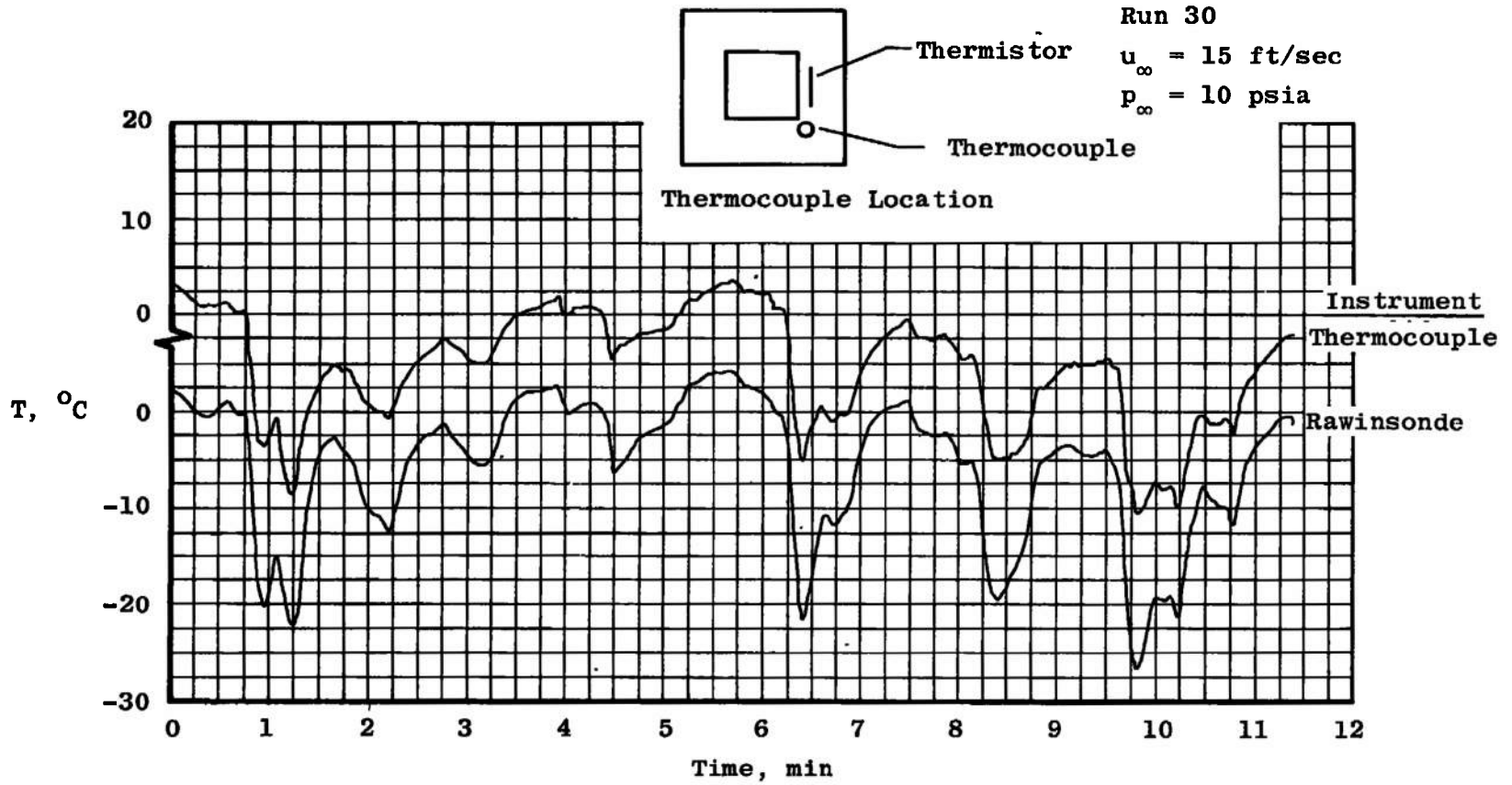
a. Thermocouple Probe Position 1

Fig. 20 Comparison of Rawinsonde and Spherical Thermocouple Reference Probe Temperature Results
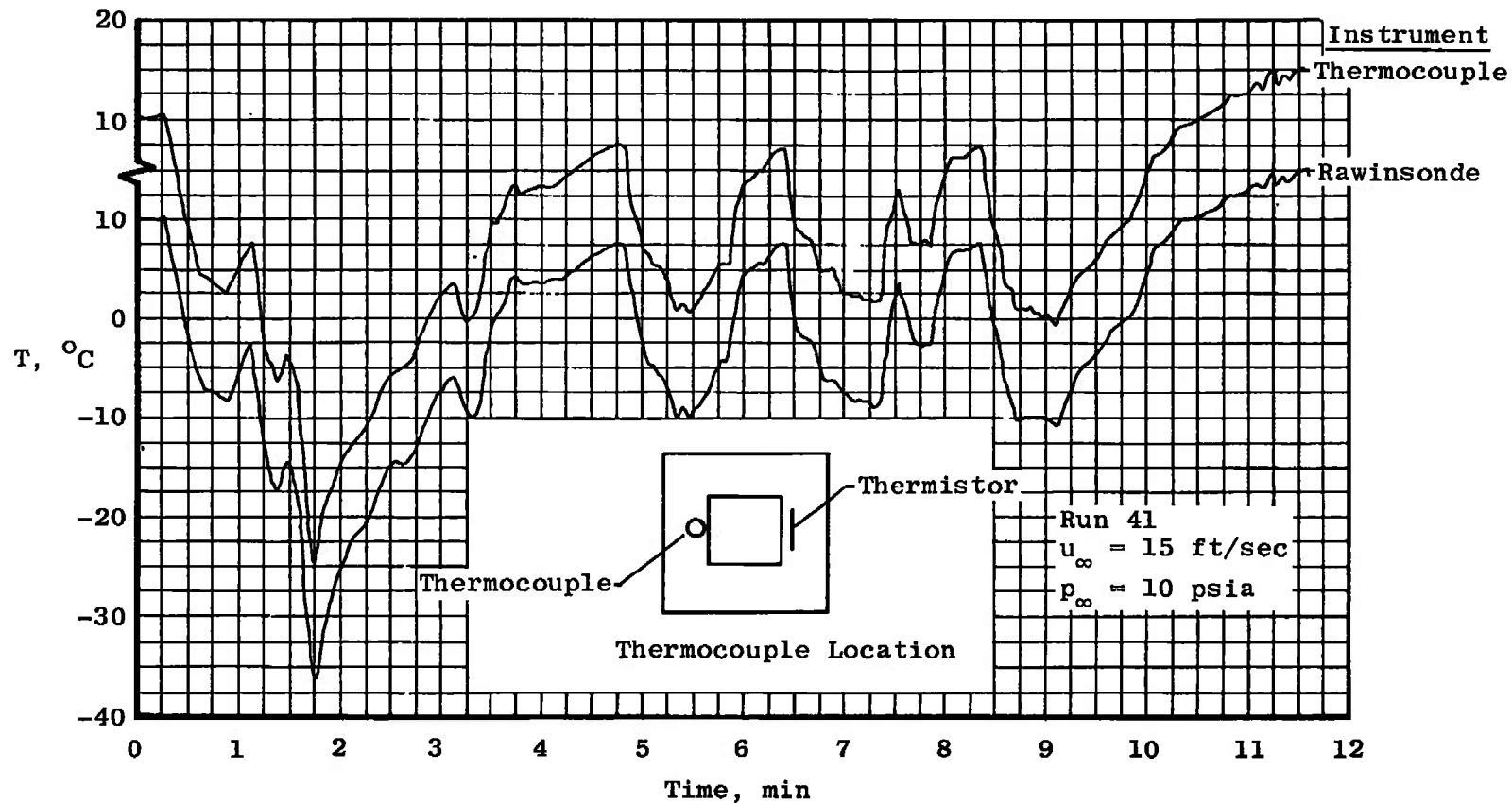
b. Thermocouple Probe Position 2
Fig. 20 Concluded
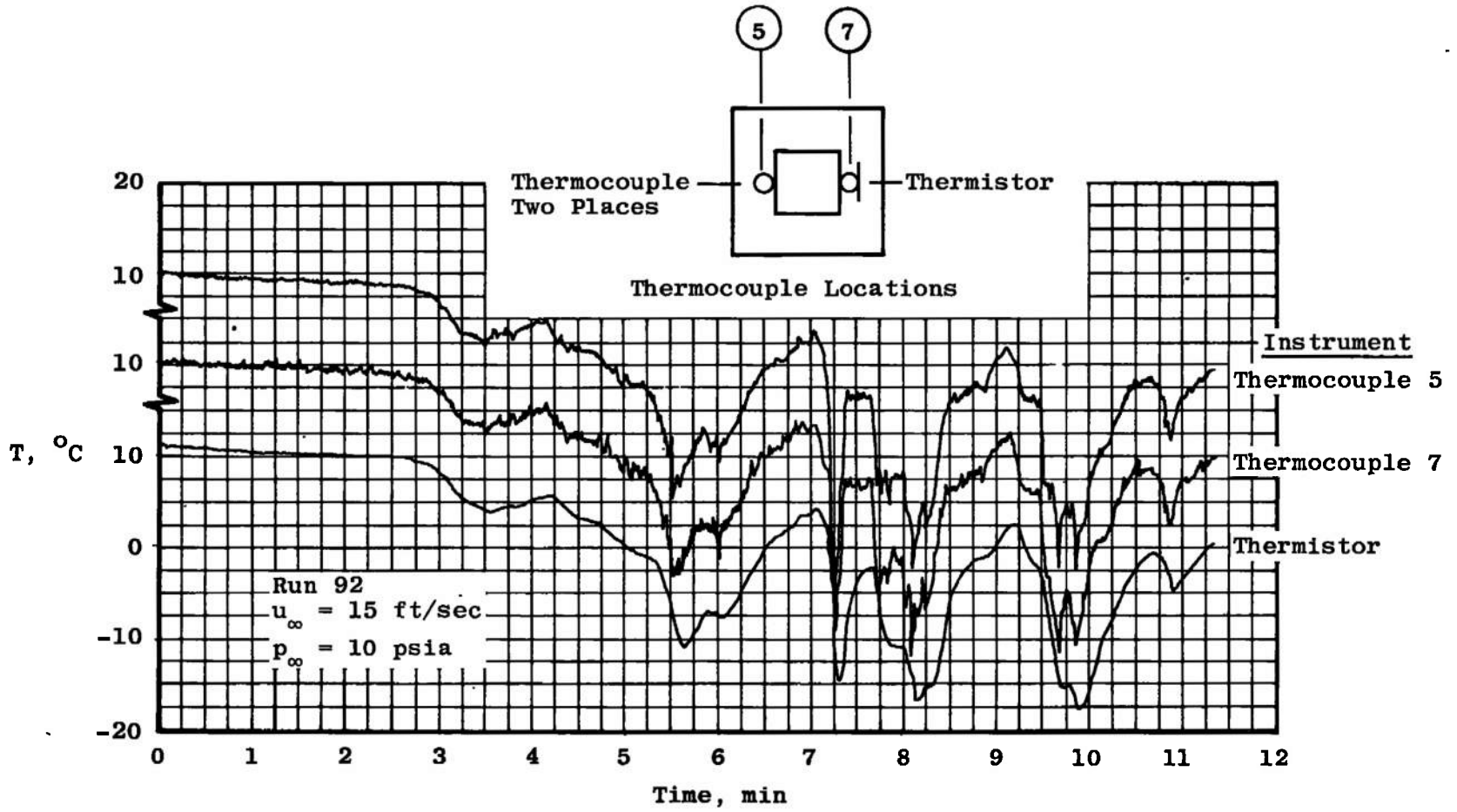
Fig. 21 Comparison of Rawinsonde and Cylindrical Thermocouple Reference Probe Temperature Results
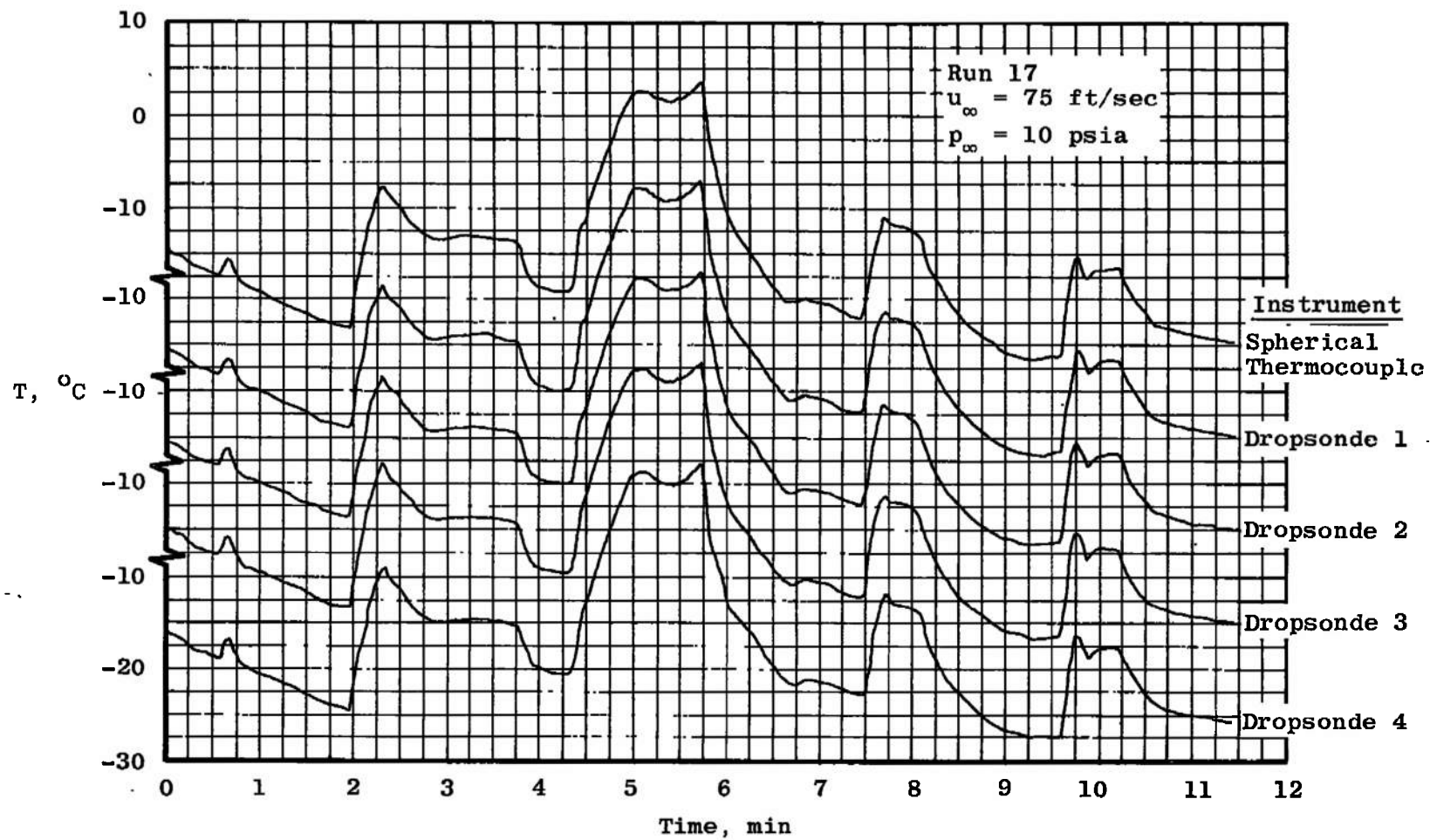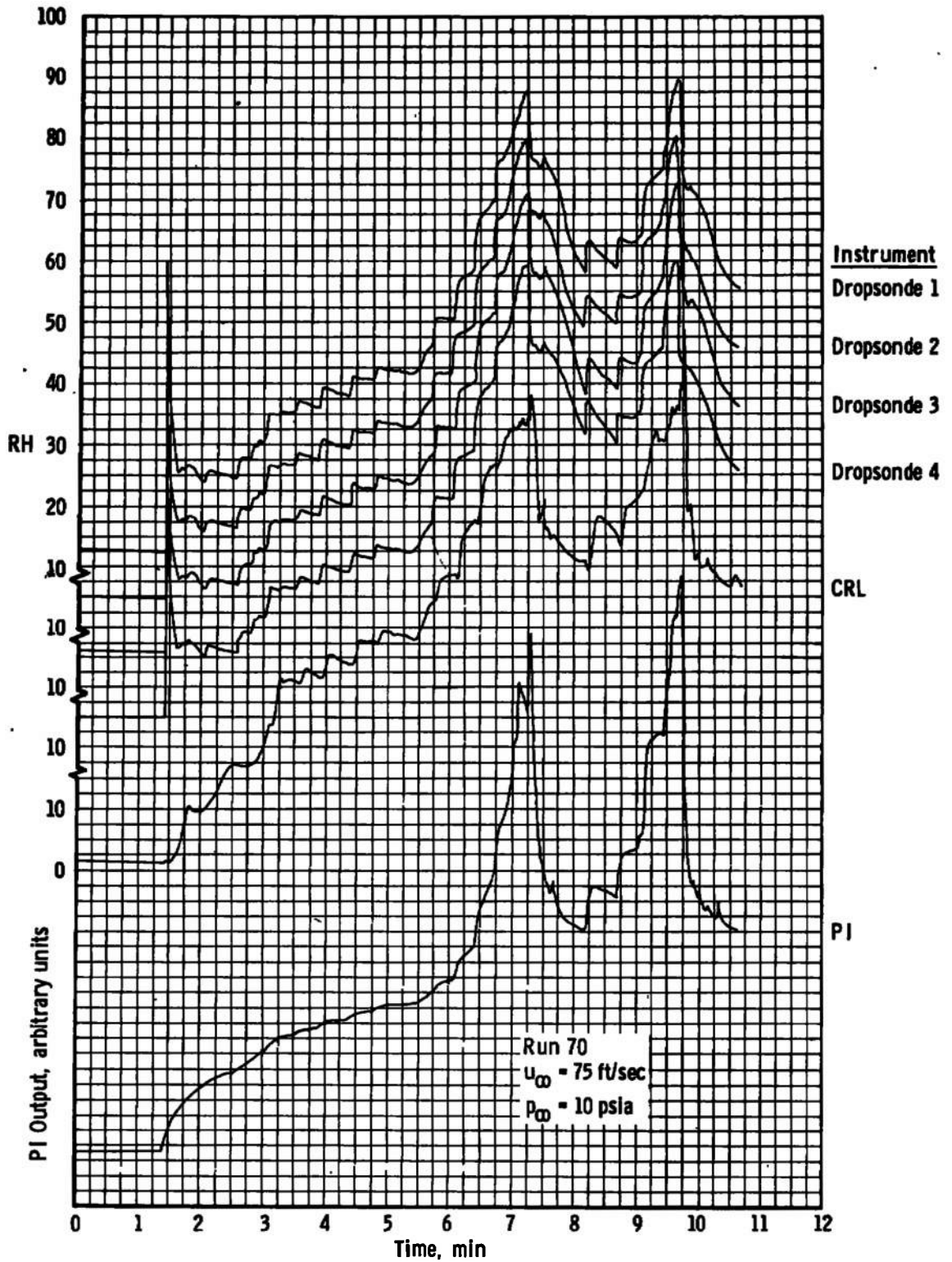
a. Without Liquid-Nitrogen Cooling
Fig. 22 Comparison of Dropsonde - ML476 Hygristor and Wind-Tunnel
Relative Humidity Results with Minimal Free-Stream Precipitation
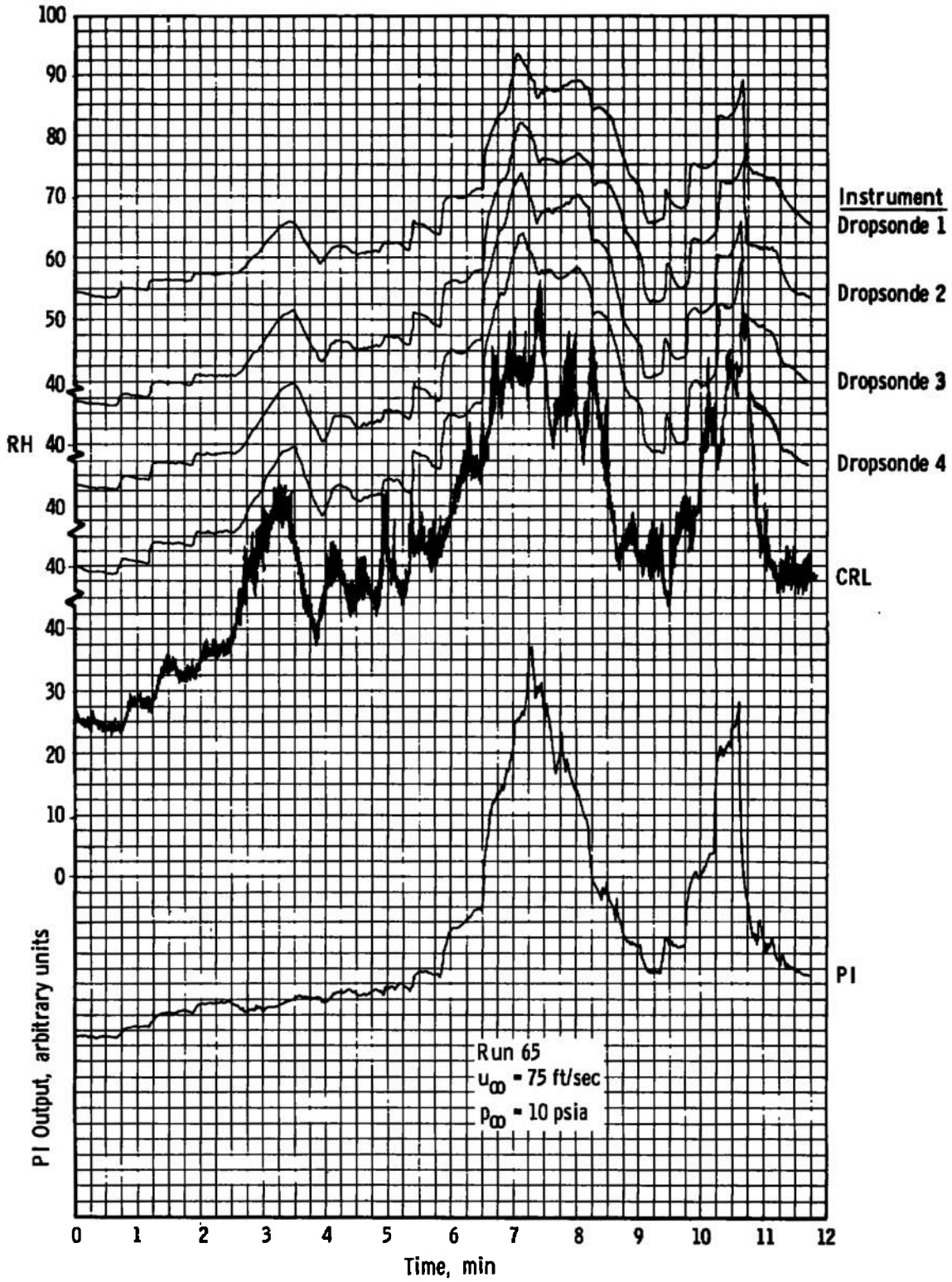
b. With Liquid-Nitrogen Cooling
Fig. 22 Concluded
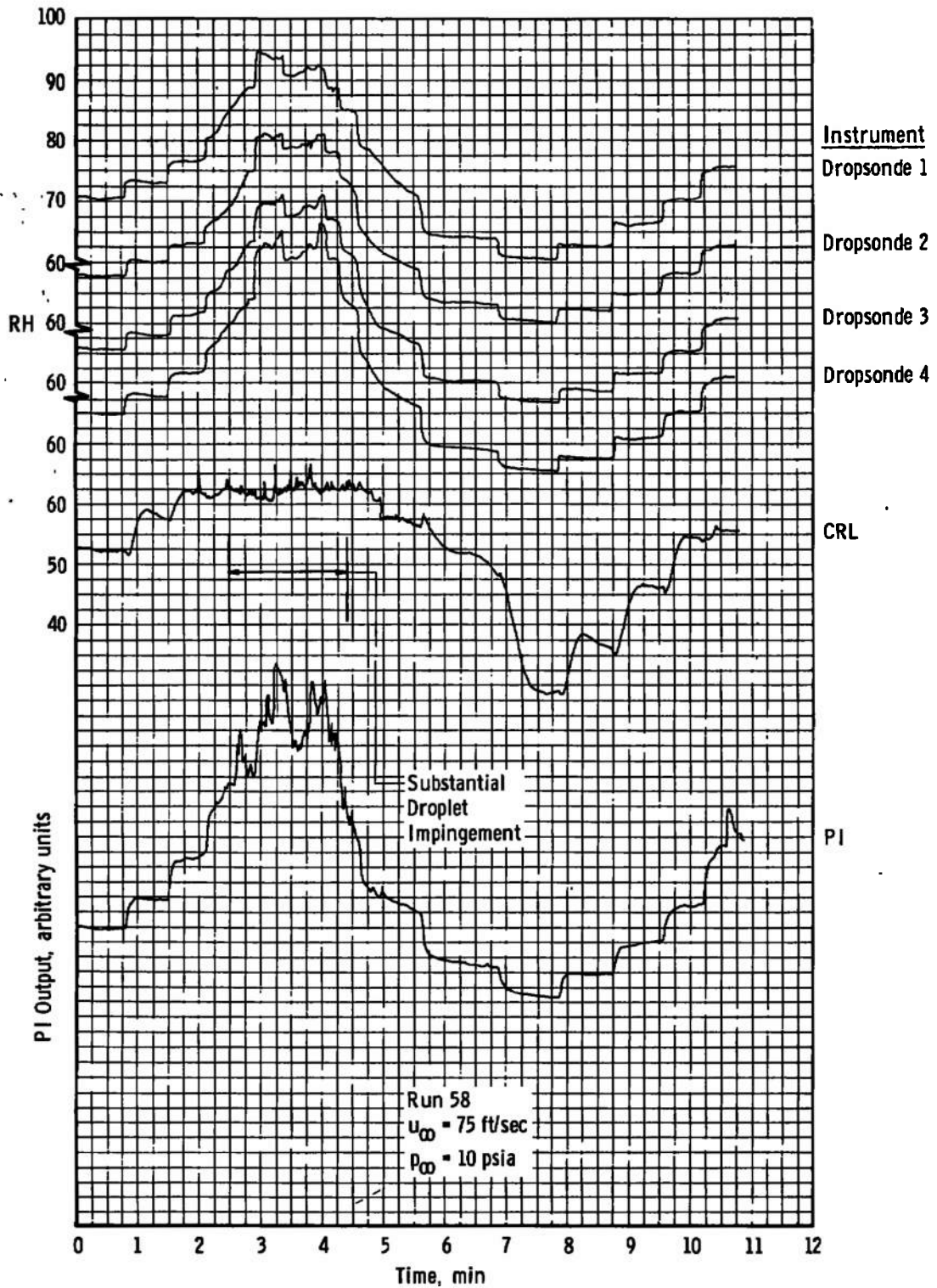
Fig. 23 Comparison of Dropsonde - ML476 Hygristor and Wind-Tunnel Relative Humidity Results with Moderate Intensity Free-Stream Precipitation

Fig. 24 Comparison of Dropsonde - CM Hygristor and Wind-Tunnel
Relative Humidity Results

a. With Droplet Impingements
Fig. 25 Effect of an Improvised Precipitation Shield on Dropsonde Performance

b. Without Droplet Impingement
Fig. 25 Concluded

a. Normal Baseline Calibration
Fig. 26 Rawinsonde Relative Humidity Results

b. Wind-Tunnel Baseline Calibration
Fig. 26 Concluded

TABLE I
SUMMARY OF TEST CONDITIONS AND SIGNIFICANT CHARACTERISTICS OF
RADIOSONDE AND WIND-TUNNEL PERFORMANCE

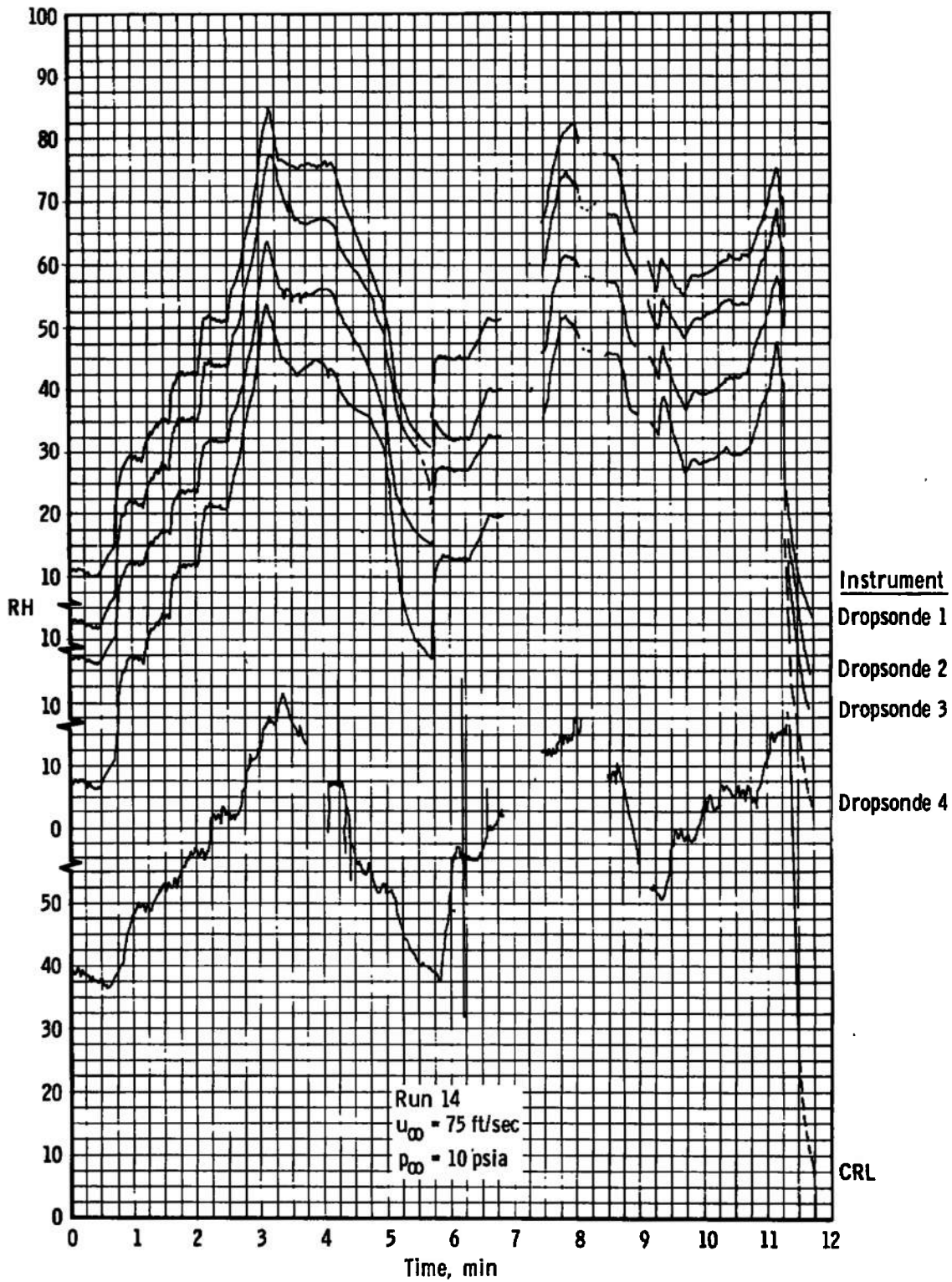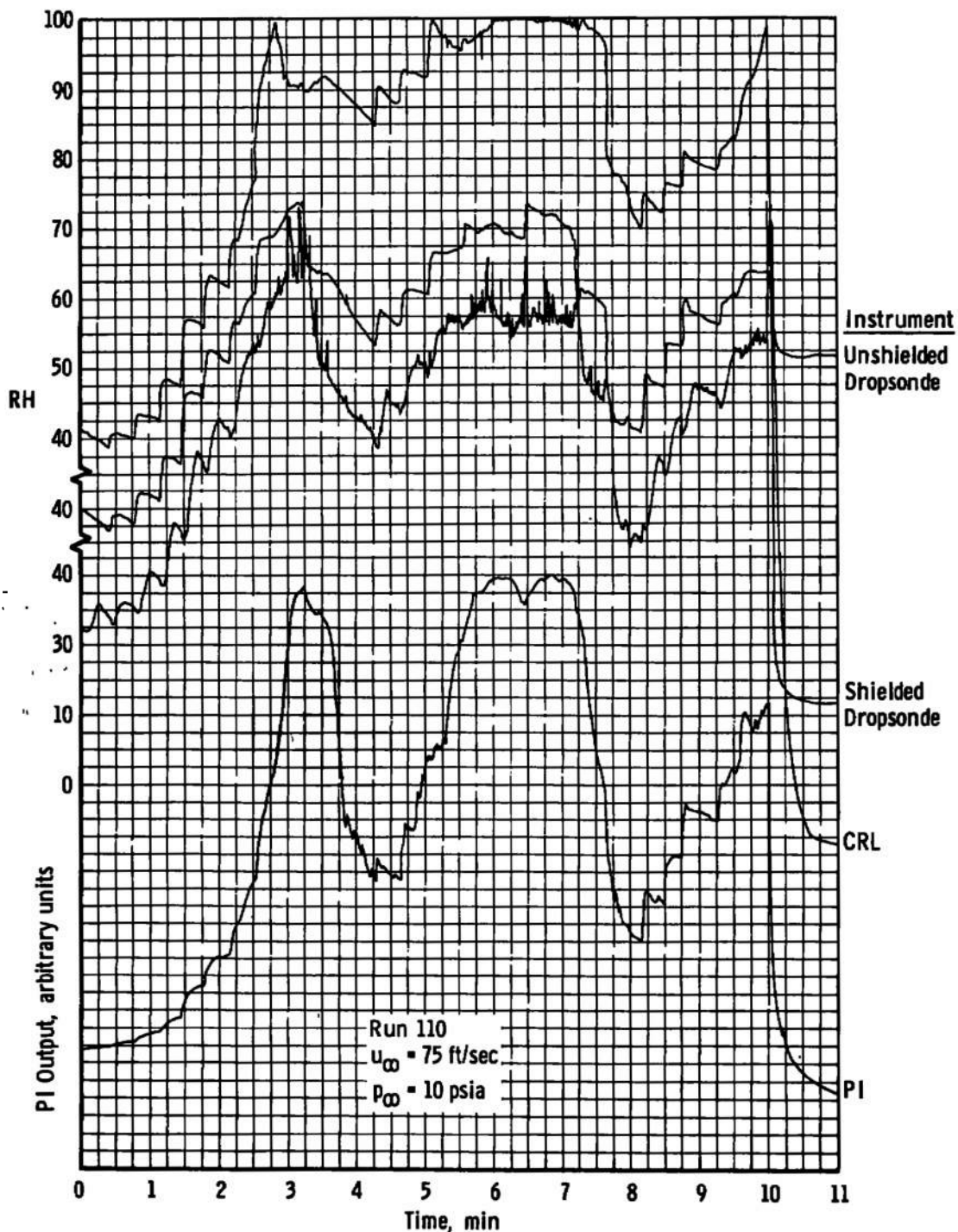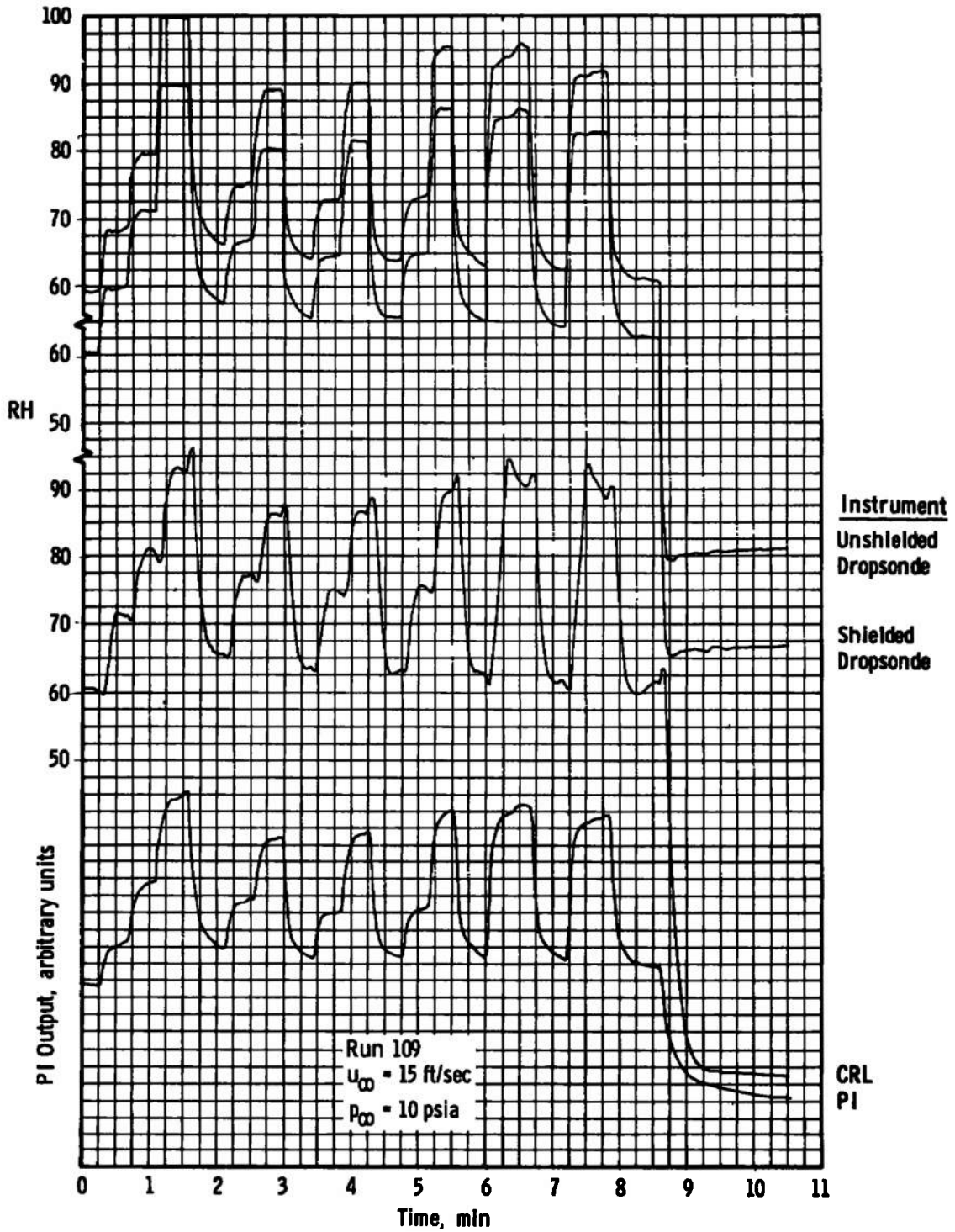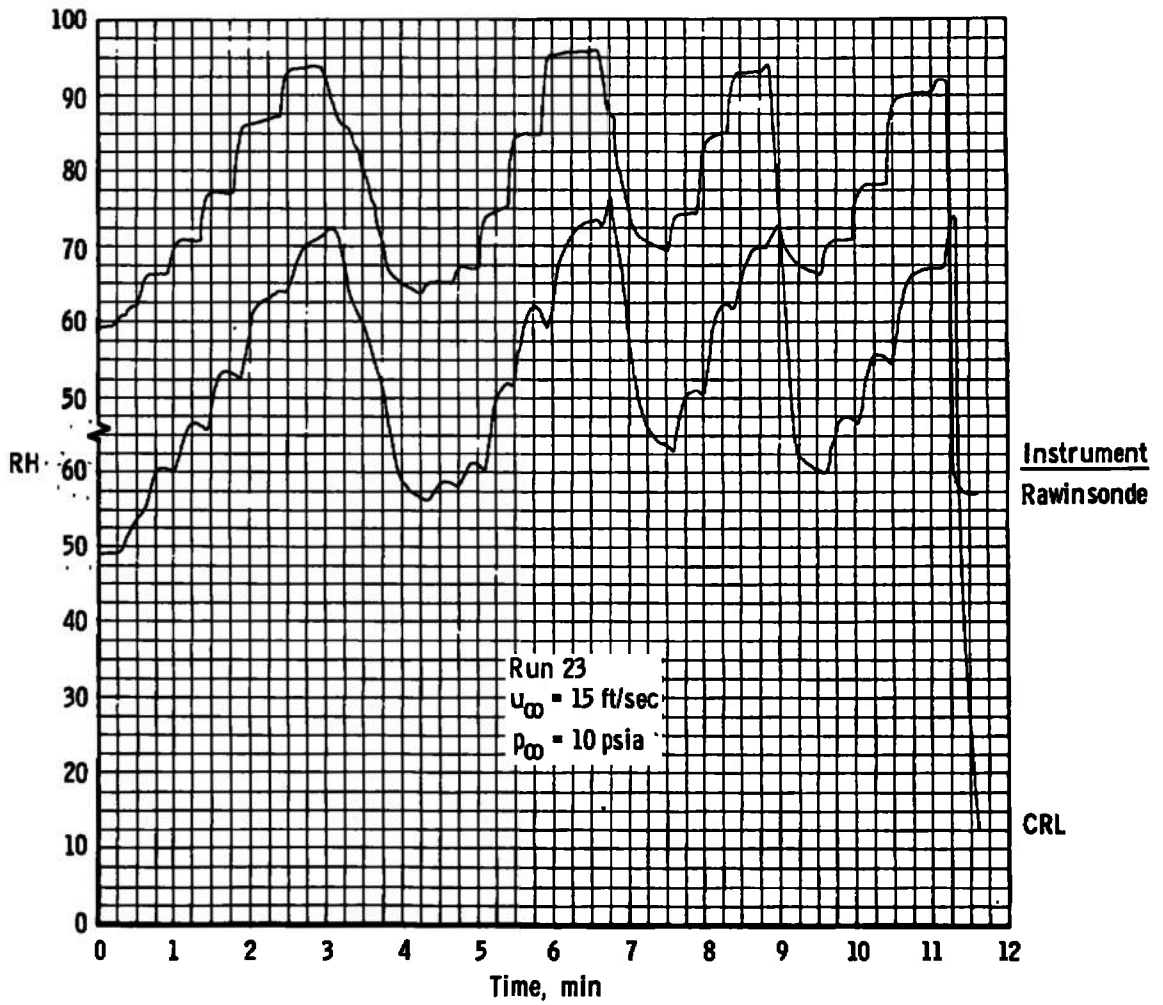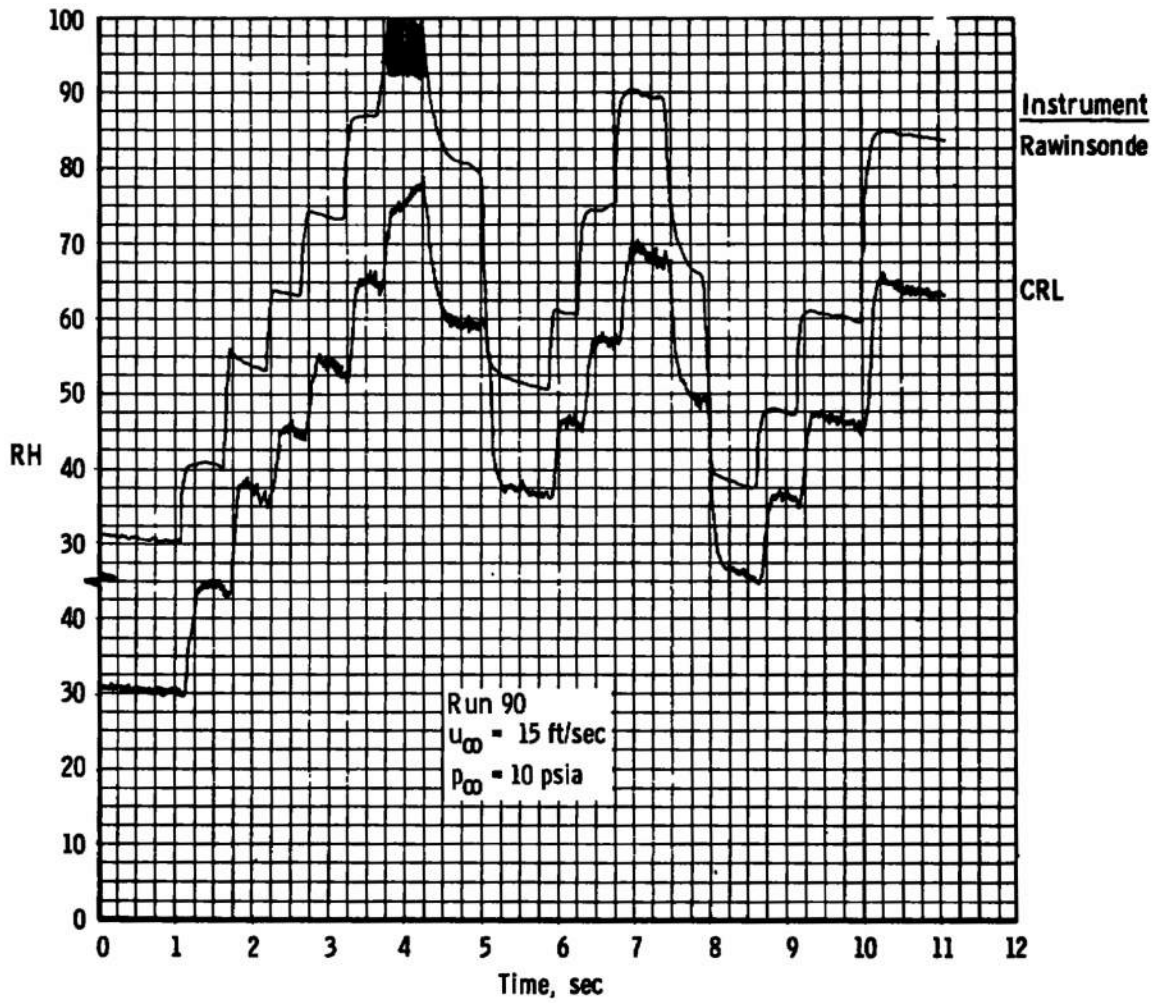| Type Radiosonde	Run No.	Radiosonde Set No.	p_∞	u_∞	T_∞	RH_∞	Measured Radiosonde Parameter	Remarks
Dropsonde	2	1	10.0	75	0/20	low[1]	T	
	3	1			-15/5	low	T	
	4	2			30	40/85	RH	
	5	2			7/25	60/100+	RH	3, 4
	6	2			-10/30	low	T	
	7	3	4.35		10	10/95	RH	4
	8		4.35		0/15	30/100	RH	4
	9				-40/5	low	T	
	10				-35/-15	low	T	
	11	4a[2]			20	5/100+	RH	
	12	4a			25	50/95	RH	3
	13	4b	10.0		30	20/75	RH	
	14	4b	10.0		20	30/85	RH	4
	15	4b	4.35		15	5/50	RH	4
	16	4	10.0		-15/30	low	T	
	17	4			-30/5	low	T	
	18	4			-25/10	low	T	
Rawinsonde	21	5	10.0	15	20	10/90	RH	
	22				20	40/95	RH	
	23				25	50/95	RH	
	24				-10/20	low	T	
	25				-10/20	low	T	
	26				-30/15	low	T	
	27	6			25	20/90	RH	
	28				25	40/95	RH	
	29				35	40/100	RH	
	30				-20/5	low	T	
	31				-40/5	low	T	
	32				-30/5	low	T	
	33	7			25	5/90	RH	
	34				25	20/90	RH	
	35				25	20/90	RH	
	36	7			-5/25	low	T	
	37				-5/25	low	T	
	38				-20/10	low	T	
	39	8			-30/20	low	T	
	40	8			-35/15	low	T	
	41	8			-30/15	low	T	
Dropsonde	50	9	10.0	75	30	30/80	RH	
	51				30	low	T	
	52				30	low	T	
	53				30	10/70	RH	
	54				10-15	20/80	RH	4
	55				0/30	0/100+	RH	4
	56	10			25+	30/90	RH	3
	57				30-	20/80	RH	3
	58				30+	30/95	RH	3
	59				30	0/100+	T	
	60				-15/35	low	T	
	61				-20/20	low	T	
	62				-40/30	low	T	
	63	11			30	5/80	RH	
	64				35-	20/90	RH	
	65				25	25/100	RH	4
	66				25-	40/100	RH	4
	67				-20/25	low	T	
	68				-15/15	low	T	
	69				-20/20	low	T	

TABLE 1 (Concluded)

Type Radiosonde	Run No.	Radiosonde Set No.	P_∞	u_∞	T_∞	RH_∞	Measured Radiosonde Parameter	Remarks
Dropsonde	70	12	10.0	75	25	5/90	RH	
	72				30-	40/95	RH	
/	73				30-	40/95	RH	
	74				30	40/95	RH	
	75				30	100/0	T	
	76				-20/25	low	T	
	77				-30/15	low	T	
	78				-40/15	low	T	
	79				-45/30	low	T	
	80	13	4.35		10-	30/6	RH	
	81				15+		RH	
	82				20-	20/90	RH	
	83				25-	30/100	RH	
	84				25-	100/0	RH	
	85				-50/0	low	T	
	86				-40/5	low	T	
	87				-20/20	low	T	
Rawinsonde	89	14	10.0	15	10-	10/95	RH	
	90				15-	30/95	RH	
	91				15+	10/95	RH	
	92				-20/15	low	T	
	93				-30/10	low	T	
	94				-35/20	low	T	
	95	15			20+	10/95	RH	
	96				25	50/95	RH	
	97				25	50/95	RH	
	98				25+	60/100	RH	
	99				25+	60/100	RH	
	100				-25/15	low	T	
	101				-30/20	low	T	
	102				-25/25	low	T	
	103	16			10-	20/100	RH	
	104				15+	25/100	RH	
	105				20-	50/100	RH	
	106				0/20	low	T	
	107				-15/15	low	T	
Dropsonde	108	17a	10.0	15	20	25/100	RH	5
	109	17a		15	20+	60/100	RH	5
	110	17a		75	30	30/90	RH	5
	111	17b		75	35-	30/80	RH	5
	112	17b		75	35	30/75	RH	5

Remarks

1. "Low" denotes minimum absolute humidity with no steam injection. Two numbers represent range of values.
2. Letter denotes change in humidity element only between runs.
3. Moderate intensity water droplets observed.
4. Nominally constant free-stream temperature controlled with liquid nitrogen during steam injection.
5. Two dropsondes installed, one employing precipitation shield.

Notes   Analog data recording used for runs 1 through 6.

CM dropsonde hygristor elements, spherical thermocouple probe, and the CRL humidity instrumentation were employed for runs 1 through 41.

ML-476 dropsonde hygristor elements, cylindrical thermocouple probes, and both CRL and PI humidity instrumentation were employed for runs 50 through 112.

Four dropsondes were tested simultaneously during each run unless otherwise noted.

DOCUMENT CONTROL DATA - R & D		
(Security classification of title, body of abstract and indexing annotation must be entered when the overall report is classified)		

1. ORIGINATING ACTIVITY (Corporate author)	2a. REPORT SECURITY CLASSIFICATION
Arnold Engineering Development Center	UNCLASSIFIED
ARO, Inc., Operating Contractor	2b. GROUP
Arnold Air Force Station, Tennessee	N/A

3 REPORT TITLE

ENVIRONMENTAL TESTS OF METEOROLOGICAL RADIOSONDES INCLUDING DYNAMIC
TEMPERATURE AND HUMIDITY SIMULATION IN A WIND TUNNEL

4. DESCRIPTIVE NOTES (Type of report and inclusive dates)
Final Report - September 23 to November 20, 1970

5. AUTHOR(S) (First name, middle initial, last name)

R. S. Hiers, ARO, Inc.

6. REPORT DATE	7a. TOTAL NO. OF PAGES	7b. NO. OF REFS
June 1971	64	0

8a. CONTRACT OR GRANT NO. F40600-71-C-0002	9a. ORIGINATOR'S REPORT NUMBER(S)
b. PROJECT NO.	AEDC-TR-71-99
c. Program Element 35111F	9b. OTHER REPORT NO(S) (Any other numbers that may be assigned this report)
d.	ARO-VKF-TR-71-46

10. DISTRIBUTION STATEMENT

Approved for public release; distribution unlimited.

11. SUPPLEMENTARY NOTES	12. SPONSORING MILITARY ACTIVITY
Available in DDC	Air Weather Service (DM) Scott AFB, Illinois 62225

13. ABSTRACT   An experimental investigation of the performance of meteoro-
logical radiosondes subjected to controlled variations of humidity and
temperature in an environmental wind tunnel is described. Dynamic varia-
tions in temperature between -60 and 40°C and in relative humidity
between 0 and 100 percent, representative of those encountered in
atmospheric flight were simulated by injecting liquid nitrogen or steam,
respectively, into the wind-tunnel air supply. Tests were conducted at
free-stream velocities of 15 and 75 ft/sec duplicating the average
ascent and descent rates, respectively, of balloon-borne rawinsondes and
dropsondes. Free-stream static pressures appropriate to the 300- and
700-mb levels were employed. Results showed that radiosonde temperature
instrumentation was generally quite accurate. Corresponding humidity
instrumentation also yielded satisfactory results except in the presence
of direct water droplet impingement or operational equipment malfunction.

DD FORM NOV 65 1473

14. KEY WORDS	LINK A		LINK B		LINK C	
	ROLE	WT	ROLE	WT	ROLE	WT
environmental tests						
meteorological radiosondes						
dropsondes						
humidity simulation						
wind tunnel						
hygrometer						
thermistor						